OPEN ACCESS Freely available online

Journal of Chemical Engineering &
Process Technology

Research Article

Effect of Different Condition Such as Coagulation Bath Temperature, Different Additive, Concentration of Polymer and Solvent on the PVDF Membrane Morphology

Mohammad Khosravi*

Department of Chemical Engineering, University of Tehran, Tehran, Iran

ABSTRACT

This paper is focused on investigating the effect of various parameters on the phase separation step on the structure and morphology of membranes fabricated from polyvinylidene fluoride. The studied parameters are PVDF polymer concentration (15-30 wt.%), solvent types including dimethyl acetamide, dimethylformamide, and normal methyl pyrrolidine, different additives such as lithium chloride, polyethylene glycol, acetic acid, methanol, and glycerol, and coagulation bath temperature (5-65°C). Scanning electron microscopy is used to examine membrane morphology. For investigating the effect of additive, three-phase diagrams are shown in the presence of dimethyl acetamide solvent. Various tests including pure water flux, effective surface porosity, maximum pore at the membrane surface, mean membrane pore size, and nitrogen penetration, have been performed on each membrane with additive and dimethyl acetamide solvent. The results proved that coagulation bath temperature, solvent type, and polymer concentration, as well as the presence of additives in the membrane solution, leads to considerable change in the membrane morphology, as clearly shown by SEM images. Adding additives to the dense layer of the membrane increases the porosity and the size of the pores, which increases the tensile strength of the membranes. Among the considered additives, glycerol and polyethylene glycol lead to the highest increase in the viscosity of polymer solution. Furthermore, the results substantiated that the presence of the additive leads to an increase in the porosity of the membrane and a decrease in the contact angle. From the pure water flux test, it was concluded that with increasing the additives, the membrane structure has changed towards higher degree of hydrophilicity. Also, nitrogen penetration test showed that the membrane porosity increases with increasing the additive, and this increment in porosity is more significant for acetic acid compared to other additives.

Keywords: PVDF membrane; Morphology; Pore forming additives; Coagulation bath temperature; Different solvent

INTRODUCTION

Among the available raw materials using for membranes fabrication, PVDF has attracted a lot of attention due to its unique properties such as high mechanical strength, thermal stability, chemical resistance, and higher hydrophobicity compared to other commercial polymer materials. PVDF membranes are widely used in ultrafiltration and microfiltration for general separations and have recently been used to make membrane contactors [1-4]. Extensive studies have been performed on PVDF membranes since 1980 [5-9] using PVDF membranes in distillation, contactors, and filtration. However, fabricating PVDF membranes with excellent performance is difficult and leads to many studies that result in fabricating membranes in the two forms of tubular and flat sheets. However, special emphasis is placed on the effect of variable parameters for membrane preparation by the phase separation approach.

In recent years, PVDF has become very popular for membrane fabrication [10]. It has more hydrophobicity compared to other

Correspondence to: Mohammad Khosravi, Department of Chemical Engineering, University of Tehran, Tehran, Iran, Tel: 9184306695; E-mail: mohamadkhosravi95@gmail.com

Received date: December 13, 2021; **Accepted date:** December 27, 2021; **Published date:** January 03, 2022

Citation: Khosravi M (2022) Effect of Different Condition Such as Coagulation Bath Temperature, Different Additive, Concentration of Polymer and Solvent on the PVDF Membrane Morphology. J Chem Eng Process Technol. 13:311.

polymeric materials such as polysulfone (PS), polyethersulfone (PES), and polyimide (PI). However, it may not be as hydrophobic as polypropylene (PP) and polytetrafluoroethylene (PTFE). Hydrophobicity of materials is often related to their surface tension [8]. Due to the complexity of material selection for membrane fabrication as well as chemical instability in case of contact with different solvents of PP and PTFE materials, the phase separation method is rarely employed. Accordingly, PVDF is the best choice for distillation membranes and contactor membranes [11]. However, as mentioned earlier, due to the excellent thermal stability of PVDF, this material has been used as a raw material for membrane fabrication in many industrial applications. Due to its low tensile strength, it is introduced as a pure polymer, which makes it suitable for biotechnological applications. In contrast to other crystalline polymers, PVDF exhibits a wide range of thermodynamic self-compatibility with other polymers such as polymethyl methacrylate (PMMA) for alloy fabrication [12,13]. This property can be useful for fabricating membranes with desired properties. PVDF can also be chemically modified with some functional groups [14,15]. It can also form cross-links when exposed to electron or gamma radiation [16].

The following table presents some references examining the membrane morphology affected by various parameters such as coagulation bath temperature, PVDF polymer concentration, the type of solvent, and various additives in the polymer solution. Some previous research studies about PVDF membrane are presented in Table 1.

Table 1: Summary of effects of the different conditions on membrane structures.

Paper	Authors	References	Conclusion
Casting and performance of polyvinylidene fluoride based membranes	Munari S, Bottino A,Capannelli G	[5]	Finger-like cavities are generated in the membrane using Binary solutions of polymer and solvent. The top surface and the bottom surface of the studied membrane showed dense skin-layer and sponge-like structure, respectively. Also, the top surface and bottom surface of the membrane corresponding to the air solution interface of the cast solution and the glass-solution interface, respectively. By increasing the polymer concentration and the reduced viscosity of the casting solutions, the size of finger-like cavities decreases. Finger-like structure or sponge-like structure can be obtained in the membrane using ternary solutions (polymer +solvent+cosolvent) by considering the cosolvent, the polymer concentration, and the period of evaporation prior to the phase inversion.
Effect of polymer concentration on the structure and performance of polyetherimide hollow fiber membranes	Gh. Bakeria, AF Ismaila, M. Shariaty-Niassarb, T Matsuur	[1]	By raising the concentration of polymer in the casting dope, the effective surface porosity, mean pore size, and membrane permeance decrease, which is due to the increase of membrane density and reduction of void fraction.
Effect of PVDF concentration on the morphology and performance of hollow fiber membrane employed as gas-liquid membrane contactor for CO_2 absorption	Nayef Ghasem , Mohamed Al-Marzouqi, Ali Duidar	[17]	The SEM result of the outer surface structures of three fabricated PVDF membranes (28%, 32%, and 34% PVDF) Presents a dense skin layer with a high concentration of PVDF.

				Intersecting polygonal plates with clear boundaries compose the skin layer. With increasing PVDF concentration in the dope solution, the size of the polygonal plates decreases. The mean Thickness of dense skin layer was reported as 11, 20, and 27 μm, for 30%, 32%, 34% PVDF, respectively. It was not reported any membrane dense skin layer for the 28% PVDF. The structure of membrane spherulites at the inner surface is almost identical, and all membranes present a high porosity.
Effects of PVDF concentration on the properties of PVDF membranes	E Pramono, AL Simamora, CL Radiman, D Wahyuningrum	[18]		The morphology of the surface and cross-sections of two types of PVDF membranes was investigated. It was shown that from the morphological aspect, there was an insignificant difference between 15 % and 17 % PVDF membranes, although there was a considerable difference in the pore dimensions of the membrane surface. They reported 55 to 110 nm on the 15 % PVDF membrane; however, the pores of the 17 % PVDF membrane have not been reported. Moreover, it was shown that high PVDF concentration in membranes leads to denser membranes with lower permeability and higher permselectivity.
Effects of Additives and Coagulant Temperature on Fabrication of High Performance PVDF/Pluronic F-127 Blend Hollow Fiber Membranes via Nonsolvent Induced Phase Separation	Chun Heng Loh and Rong Wang	[19]		The cross-sectional morphology of fibers spun at a coagulation temperature of 25 °C, and 40 °C was investigated. In this regard, the effects of coagulation temperature on macro-void formation were reported as well. Considering a higher coagulant temperature during the spinning process resulted in a smaller size of macro-voids developed below the outer surface of the fibers. Additionally, it was observed that at a coagulant temperature of 40 °C, the sponge-like structure area close to the lumen of the fibers increases in comparison to when the coagulant temperature is 25 °C. They showed that the thermodynamic stability of a polymer dope system is improved at a higher temperature, resulting in a lower polymer precipitation rate.

Effect of Temperature on the Formation of Microporous PVDF Membranes by Precipitation from 1-Octanol/DMF/PVDF and Water/DMF/PVDF Systems	Liao-Ping Cheng	[20]	The effect of temperature on membrane morphology was studied. They showed that the membrane composed of spherical PVDF crystallites of roughly identical size and fabricated at 25 °C is uniform in all dimensions. Also, the cellular structure that identifies the liquid-liquid demixing in precipitation was not observed. However, the membrane formed at 65 °C was asymmetric with a dense layer formed on the upper surface, and a cellular structure mixed with spherical particles was observed on the membrane cross-section. The differences in membrane morphology for these two membranes can be described by the phase behaviors at the considered temperatures.
Effects of Coagulation Bath Temperature on the Separation Performance and Antifouling Property of Poly(ether sulfone) Ultrafiltration Membranes	Jinming Peng, Yanlei Su, Wenjuan Chen, Qing Shi, and Zhongyi Jiang	[21]	PES ultrafiltration membranes were formed at CBT spanning from a temperature of 20 to 60 °C. The cross-section morphologies of the fabricated PES membranes were studied with SEM, and all of the membranes presented the typical asymmetric morphology with a thin skin layer on upper surface and a porous bulk at the bottom surface. The permeation and rejection of solutes correspond to the skin layer, while the bulk plays as mechanical support. A finger-like intermediate layer and fully developed macro-voids were observed for the porous bulk of PES/PEG membranes.
Effect of Coagulation Bath Temperature on Formation Mechanism of Poly(vinylidene fluoride) Membrane	Xuyun Wang, Lin Zhang, Dahai Sun, Quanfu An, Huanlin Chen	[22]	It was observed that using a lower coagulation bath temperature increases the transparence of the membrane as well as the shrinkage ratio of the membrane. In this regard, the shrinkage ratios of the membranes fabricated in the coagulation temperature of 60 °C, 25 °C, and 15°C were 10.0%, 61.4%, and 73.5%, respectively. In terms of the variation of thickness and porosity with coagulation bath temperature, it was reported that the membrane fabricated at 60 °C de-ionized water shows a considerable increase in the thickness and porosity compared with membranes fabricated at a lower temperature.

Effects of Coagulation Bath Temperature and Polyvinylpyrrolidone Content on Flat Sheet Asymmetric Polyethersulfone Membranes	M Amirilargani, E Saljoughi, T Mohammadi, MR Moghbeli	[23]		From cross-sectional SEM images of the membrane fabricated at 0 °C as a coagulation bath temperature, an asymmetric spongy-like structure in the sublayer was observed. Also, it was reported that a denser skin layer can be resulted from preparing the membrane at a coagulation bath temperature of 80C. By increasing the coagulation bath temperature, the sublayer structure of the membrane changed from a spongy-like structure to fully develop finer pores, and the surface pores size of the membrane increased as well. Also, it was concluded that at rapid precipitation conditions, micro-voids formation is happened, which leads to faster precipitation at higher temperatures. Nucleation was observed after a specific time with considering slow demixing, and the membrane top layer included high polymer concentration. Then, nucleation is successively initiated in the subordinate layer at short time intervals. Therefore, new nuclei are gradually formed near nuclei in the former layer.
Effect of additives in the casting solution on the formation of PVDF membranes	Enrica Fontananovaa, Johannes. Jansena, Alessandr Cristianoa, Efrem Curcio , Enrico Drioli,	[24]		This study focused on investigating the thermodynamic/kinetic effects of hydrophilic additives during the phase inversion process for preparing PVDF-based membranes. LiCl and PVP were considered as additives that are soluble in DMA and H_2O, and are leachable by exchanging with a coagulation bath. Using PVP in the casting solution improved the accentuation and extension of macro voids presented in PVDF homopolymer in the cross-section of membrane. However, the micro void formation became lower considering a high LiCl concentration. This different behavior can be described by the opposing effects of additives on thermodynamic and kinetic during the phase inversion process. Both PVP and LiCl decrease the thermodynamic miscibility of the casting solution and improve liquid-liquid phase separation. On the other hand, phase separation delay occurs due to the increase of solution viscosity and delay of mutual diffusion between solvent

				in the coagulation bath and non-solvent in the cast film.
Study on the effect of a non-solvent additive on the morphology and performance of ultrafiltration hollow-fiber membranes	M Khayef, CY Feng, KC Khulbe, T Matsuura	[25]		It was observed that the addition of ethanol leads to a delay in the coagulation process, which resulted in the change of structure from finger-like to sponge-like. By increasing the concentration of 1, 2-ethanediol in the spinning solution, the mean pore size increases, while the effective porosity of all hollow fibers prepared from the spinning solutions containing non-solvent additive was almost identical and was larger than the effective porosity of the membrane.
Effect of additives concentration on the surface properties and performance of PVDF ultrafiltration membranes for refinery produced wastewater	E Yuliwati, AF Ismail	[26]		The FESEM micrographs of the cross-sectional morphology of the fabricated PVDF UF membranes showed that increasing the PVDF concentration between 16 to 22 wt % brings about a considerable change in morphology and prevents the formation of finger-like structure macro voids. For PVDF concentration of 22 wt%, the formation of finger-like structure below the top layer was significantly lower than the case of 19 wt% PVDF concentration. Also, a transition from the macroporous structure to the asymmetric structure in the membrane cross-section was observed. Moreover, a thicker top layer of the membranes with a more sponge-like substructure was formed across the membrane wall. This is mainly because of high dope viscosity that reduces the solvent and non-solvent exchange rates and increases the resistance of diffusion from the polymer aggregation.
Effects of Additives on the Morphology and Performance of PPTA/PVDF in Situ Blend UF Membrane	Hong-Bin Li, Wen-Ying Shi ,Yu-Feng Zhang ,Dong-Qing Liu and Xiao-Feng Liu	[27]		The thermodynamic and kinetic properties of casting solution were analyzed, and it was proven that with raising the PEG concentration from 0 to 6 wt%, solution viscosity gradually increases, and thermodynamic stability slowly decreases. Also, It was shown that by a further increase of PEG concentration to 8 wt%, a slight decrease in gelatin values was observed, which demonstrates a slight reduction in the thermodynamic stability of the casting solution. Accordingly,

				during the immersion of casting solution in the coagulation bath, the sharp increase of solution viscosity resulted in a delay in phase separation. Also, it was observed that the porosity and water flux of the membrane can be improved by adding LiCl. In addition, a finger-like pore structure was observed by considering Tween as the additive.
Morphological Study of Poly(vinylidene fluoride) Asymmetric Membranes: Effects of the Solvent, Additive, and Dope Temperature	ML Yeow, YT Liu, K Li	[28]		Using a poor solvent such as TEP, a symmetry sponge-like structure was observed over the whole thickness of membrane, without any cavity. Because of the low solvent power of TEP, a small amount of non-solvent can induce the phase inversion of the polymer solution, leading to early occurrence of liquid-liquid phase separation and preventing macro voids formation. Also, it can be attributed to a poor mutual affinity between TEP and water compared with NMP, DMF, and DMAc, which can enhance the formation of a spongy-like structure. However, using NMP as a solvent, inconsistent macro voids were exhibited under the skin layer, which is due to inadequate time for the solvent and non-solvent exchange and the formation of a skin layer at an initial stage. Also, the presence of insufficient water in the substrate phase to induce phase inversion contributes to the formation of macro voids, which can be explained by the high hydrophobicity of the PVDF material. On the other hand, using DMF and DMAc as solvents for casting flat-sheet membranes leads to a similar shorter finger-like structure with sponge substrates, which is because of a slow exchange of solvent and non-solvent in the immersion-precipitation processes.
Effects of mixed solvents on the structural morphology and membrane distillation performance of PVDF-HFP hollow fiber membranes	L García-Fernández, MC García-Payo, M Khayet	[29]		Since DMAC is a more efficient solvent compared to DMF, using DMAC leads to a lower macro-void in the cross-section of the PVDF-HFP hollow fiber membrane. Also, using DMAC contributes to thermodynamic stability, lower coagulation rate, and higher viscosity. . Furthermore, by considering DMAC as a solvent

				instead of DMG, the solvent evaporation begins earlier. Also, the permeate flux of DCMD, as well as the factor of NaCl rejection, are improved due to a dense internal sponge-like structure, low thickness, and the high mean roughness of both the outer and inner surfaces.
The effect of different solvents on the morphology and performance of the ZIF-8 modified PVDF ultrafiltration membranes	Atefeh Karimia, Alireza Khataeea, Vahid Vatanpourd, Mahdie Safarpour	[30]		It was reported that the resulted structure of the fabricated membranes was not consistent with the structure predicted by thermodynamic, which substantiated that the kinetic effect (mass transfer) of the membrane formation needs to be considered. The instantaneous liquid-liquid demixing and consequent finger-like cavities are determined by the interactions between polymer casting solvents and water as the coagulation bath. It was shown that the formation of solvent-rich local nuclei has occurred below the upper layer of the membranes. A constant number of nuclei can be achieved using a constant solution. The formation of finger-like cavities is related to the growth of the existing nuclei. The mutual diffusivities of solvent/non-solvent can be ordered as follows: DMF>DMAc>NMP>DMSO. The high diffusion rate of the solvent/non-solvent is responsible for existing many finger-like pores with a small size. It was proved that the water-NMP and water-DMSO have a lower diffusion rate compared to the water-DMAc and water-DMF, leading to a lower rate of new nuclei formation. Therefore, the total amount of new nuclei was lower, and larger finger-like pores were obtained in the sub-layer structure of the DMSO and NMP prepared membranes. A great number of small size finger-like pores were created in the membranes made from DMF and DMAc solvents due to the fast diffusivities of solvent/non-solvent.

Cheng investigated the effect of sediment temperature on the morphology and crystal structure of PVDF membranes made of (PVDF/DMF/1-octanol) and PVDF/DMF/Water systems. In this work, two coagulation baths were used at 25 and 65°C for membranes fabrication. Because the crystallization process overcomes the liquid-liquid separation at 25°C, at this temperature, a symmetrical membrane with identical spherical crystals of PVDF was formed [20]. Wang observed a similar effect to Cheng work for coagulation bath temperature on the obtained membrane crystallinity. He observed that the membrane fabricated in the coagulation bath at 15°C showed more crystallinity than the membrane fabricated in the 60 °C bath. He observed that the membrane prepared at 60°C had only α-type crystal structure. While at 15°C, the existing membrane has a combination of α and β type crystal structures [31]. Cheng showed that the presence of 1-octanol in the coagulation bath and polymer solution causes the formation of PVDF membrane using the crystallization process. He also noticed that if the crystalline process dominates the liquid-liquid separation during membrane formation, the particle size decreases with increasing the amount of 1-octanol in the polymer solution [32]. With dissolving PVDF (DMF) at different temperatures and immersing it in an octanol coagulation bath, Lin showed that the pore size in the morphology of the membrane increased with the increasing temperature of the polymer solution. However, in this crystallization experiment, all membranes remained unchanged, and all of them had α-type crystal structures [33]. Also, Wang observed significant changes in the morphology of the prepared membrane by dissolving PVDF in (DMAc) and forming a membrane in a water bath. In their studies, it was observed that the cross-section of all membranes consists of an interconnected structure with cavities in which only α phase exists in its crystal structure. In this experiment, it was observed that with increasing the temperature of the polymer solution, the size of these cavities increases [31]. Benz and Euler determined the phase compositions of crystals by measuring the degree of crystallinity of α, β and γ in PVDF thin film by infrared spectroscopy [34]. Gregorio determined three crystalline phases composed of PVDF films prepared under different conditions using Fourier transform infrared spectroscopy and X-ray diffraction [35]. Madorsky et al. have conducted extensive studies on the thermal degradation of PVDF at medium and high temperatures under vacuum conditions. Their results from vacuum thermal decomposition showed that the heat degradation mechanism in PVDF leads to the loss of hydrogen fluoride (HF) and causes various chemical reactions that form a carbon-carbon double bond (C=C)-or cross-linked polymer [36]. Nguyen has also conducted many studies on the thermal degradation of PVDF using various processes [37]. Lovinger and Reed observed heterogeneous thermal degradation of PVDF crystallized at high temperatures (about 160°C). They noticed that different spherulitic are formed in different degradation of PVDF, which causes a heterogeneous color change in the samples. These degradation processes occur in the crystalline region and have no effect on amorphous segments [38]. Furusho et al. have conducted further analysis on the thermal degradation of various halogenated polymers, including PVDF, using torsional band analysis. Among the studied halogenated polymers, PVDF showed the highest thermal stability [39]. Benzinger evaluated the thermal stability of a PVDF ultrafiltration membrane using spiral-wound measurements at a higher temperature during continuous operation at 85 ºC while keeping the temperature constant for seven months. No signs of thermal degradation of PVDF membranes were observed in that time period [40]. Nguyen has conducted a comprehensive review of the degradation of PVDF, for which minor information is still available on its degradation using alkaline solution [37]. Subsequently, some reports were released about the observations of PVDF discoloration from white to brown and then blackening during immersion in alkaline solution for a short time [41,42]. Hoa and Ouellette also showed that chemical traction could accelerate the chemical attack of sodium hydroxide on PVDF. If the amount of tensile is high enough, it can create a gap. They observed that the attack of sodium hydroxide on PVDF in solution was in the α-formulation. Also, the discoloration of the PVDF sample in this solution was detected [43]. Kise and Ogata investigated the reaction between PVDF powder and aqueous sodium hydroxide solution in the presence and absence of four-component ammonium as a phase transfer catalyst [44]. Hours after PVDF was immersed in the high-temperature solution, PVDF discoloration was observed. The reaction was also faster with the presence of ammonium bromide. In this experiment, infrared spectroscopy showed the formation of a carbon-carbon double and triple bond to remove HF molecules. Benzinger has conducted extensive researches on the effects of a variety of acids, bases, and oxidants, including sodium hydroxide, on PVDF membranes. It was observed that PVDF membranes have excellent stability against chemicals, acids, strong oxidants, and most organic solvents. However, it does not have good stability compared to a concentrated solution of sodium hydroxide that has been immersed in it for three months [40]. Similar observations have been reported by Vigo on PVDF membranes [45]. Hashim et al. have done many studies on the chemical stability of PVDF tubular membranes. They used different grades of PVDF in sodium hydroxide solution at temperatures of 20 and 70°C. They observed that different grades of PVDF have different degrees of degradation [46]. Sukitpaneenit and Chung showed the thermodynamic phase separation processes of PVDF membranes in phase diagrams [47]. Figure 1 shows the three-phase diagrams of systems (PVDF/NMP/anti-solvent) at 25 °C prepared to measure the cloud point. The gelation line for the system (PVDF/NMP/water) is closer to the polymer-solvent axis than for other systems. In other words, only a small amount of water is needed to disturb the system and the polymer tends to precipitate. The results show that the thermodynamic stability of the systems (PVDF/NMP/solvent) is as follows: Water<methanol<Ethanol<Isopropanol. Therefore, for NMP/PVDF/Water system, water is a strong anti-solvent and alcohols are weak anti-solvents [47].

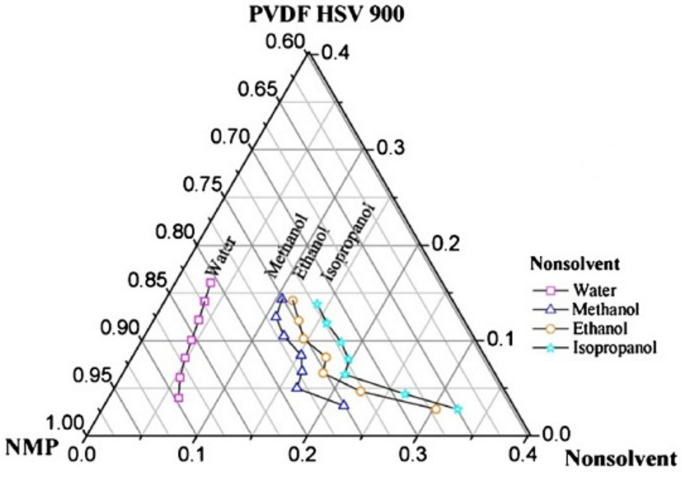

Figure 1: Shows the three-phase diagrams of systems (PVDF/NMP/anti-solvent) at 25 °C prepared to measure the cloud point [47].

As shown in Figure 2, Yeow proved that different solvents during the dispersion process of the solution on a suitable surface have a great influence on its final structure. Triethyl phosphate as a solvent and water as a coagulation bath can be used to form a symmetrical spongy structure at the cross-section of the membrane, as reported by Bottino [48] and Shih [49]. Researchers have shown that solvent strength plays a very important role in determining the morphology of the final membrane. Solvents such as DMAc, DMF and NMP are considered as strong solvents [28]. Li used a mixture of four solvents (TMP-DMAc, TEP-DMAc, TCP-DMAc and TBP-DMAc) to achieve four different structures for PVDF membranes [50]. The results of this experiment were that strong solvents such as TMP-DMAc and TEP-DMAc showed higher deposition rates, less shrinkage of the membrane and consequently higher water flux. Also, it has been observed that the membrane obtained from TEP-DMAc solvent compared to TMP-DMAc cause's smaller cavities in the dense sub-shell structure of the membrane, which lead to higher permeability and better mechanical properties.

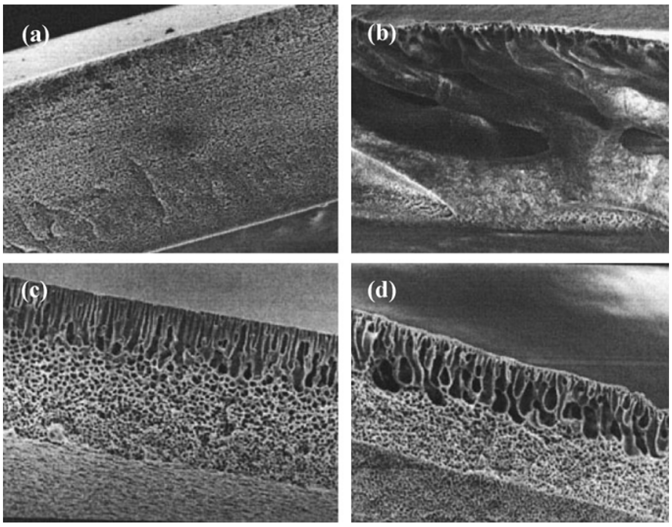

Figure 2: Different solvents during the dispersion process of the solution, such as DMAc (c), DMF (b), THF (a) and NMP (d) [28].

Munari investigated the effect of evaporation time of PVDF solution spreaded on the surface to prepare membranes from various polymer-solvent systems. In this experiment, DMF and NMP were used as a high solvent boiling point in the presence and absence of acetone or THF as a low boiling point auxiliary solvent. It was concluded that the morphology and properties of the membrane prepared from the solution containing high boiling point solvents did not have a significant effect on evaporation time. However, evaporation time affects the morphology of the membrane prepared from DMF or NMP and acetone or THF as an auxiliary solvent. Also, their mechanical properties and performance can change as one of the results of the precipitation phenomenon during evaporation [5]. Bottino investigated the effect of lithium chloride (LiCl) on the formation of PVDF membranes [51]. It was observed that the presence of LiCl in the polymer solution would have a significant effect on the morphology of the membrane. The formation of a porous structure and the presence of large cavities in the cross-section of the membrane can be some of the effects of LiCl addition. Kong and Li discovered a nonlinear increase in the viscosity of the polymer solution with increasing the amount of LiCl and the rate of the NMP-containing polymer solution increased as a solvent compared to DMAc [52]. They also observed that when polyvinylpyrrolidone is used as a hydrophilic additive, it increases the porosity and average pore size of PVDF tubular membranes. Recently, anti-solvents have been used in various experiments as additives in polymer solutions. Examples include glycerol and water. It has been reported by researchers that the addition of water as an additive to the polymer solution increases the diameter of the pores on the surface and the porosity of the final PVDF membrane [53]. In this regard, Khayet and Matsuura have shown that with increasing the amount of water in the solution, the mass transfer resistance of the PVDF membrane decreases. Also, using 1, 2-ethanediol as an additive leads to an increase in the pore size and the flux of pure water [25].In this research, a solution with different percentages of polymer 15-18-21-24-27-30 wt% of polyvinylidene fluoride (PVDF) polymer for high hydrophobicity was used as the raw material for fabricating the membrane and then the effect of different solvents such as DMF-DMAc-NMP is investigated. Also, for further morphology study, the effect of coagulation bath temperature at 5-15-25-45-55-65° C is analyzed. Furthermore, five types of additives, such as glycerol, polyethylene glycol, lithium chloride, methanol, and acetic acid, with 4 wt%, have been employed to create porosity and cavities in the membrane surface.

MATERIALS AND METHODS

Materials

To fabricate the appropriate membrane, it is needed raw materials that fit the expected morphology. Therefore, all the materials used in the research for membrane fabrication are introduced, and then the procedure to use each of them is explained.

The polymer used to fabricate the membrane in this research was polyvinylidene fluoride (PVDF) grade kynar 720 provided by the French company ELF Atochem. The polymer is in the form of granules with a molecular weight of 240,000 g/mol. Dimethyl acetamide (DMAc), dimethylformamide (DMF), and normal methyl pyrrolidine (NMP) with a purity of more than 99% made by Merck were used as a solvent for the polymer. These materials are colorless and are known as strong organic solvents for PVDF.

Also, distilled water (single distillation) was used as an anti-solvent. Lithium chloride (LiCl), polyethylene glycol (PEG 400), acetic acid, glycerol, and methanol were used as additives. All the above chemicals with the purity of more than 99% are produced by Merck Company. Pure water was used to perform the flux test. To evaluate the overall porosity of the membrane surface, 2-ethyl hexanol oil with a mass (833 g/cm^3) was employed. The reason for using this material is its high boiling point, and very good penetration in this membrane fabricated from PVDF polymer [43]. Table 2 illustrates all the materials employed in the experiments.

Table 2: Shows the chemical structure of the material used in all tests.

Chemical name	Chemical formula	Density (Kg/m3)	Boiling point (°C)	Pour point (°C)	Molecular weight (gr/mol)	IUPAC name
polyvinylidene fluoride	-(C2H2F2)n-	1780	Tg=-40	177	240000	poly(1,1-difluoroethylene)
Dimethylformamide	C3H7NO	944	153	-61	73.09	N,N-Dimethylmethanamide (DMF)
Dimethyl acetamide	C4H9NO	937	165	-20	87.12	N,N-Dimethylacetamide (DMAc)
Dimethyl pyrrolidine	C5H9NO	1028	203	-24	99.13	1-Methyl-2-pyrrolidone (NMP)
Lithium chloride	LiCl	2068	1382	610	42.39	Lithium chloride (LiCl)
polyethylene glycol	C2nH4n+2On+1, n = 8.2 to 9.1	1128	238	8	420	Polyethylene glycol (PEG)
Acetic acid	C2H4O2	1049	118	17	60.5	Acetic acid
Methanol	CH4O	791.8	64.7	-97.6	32.4	Methanol
Glycerol	C3H8O3	1261	290	17.8	92.09	propane-1,2,3-triol

Flat sheet membrane fabrication

First, the PVDF granules were placed in a vacuum oven at 60°C for 2 hours so that there was no moisture during the experiment. To prepare the polymer solutions, after the polymer was completely dissolved in the solvent at 25°C and became a homogeneous solution, it was then left in the same condition for one day until all the air bubbles in it were removed from the solution. The polymer solution is placed in an ultrasonic bath at 60°C for 90 minutes in order to homogenize and remove possible bubbles and to disperse the additives completely in the polymer solution. Then, to prepare the membranes, a flat glass plate was employed to prepare the film on it. In Figure 3, the automatic film maker used in this study has been shown which has the ability to adjust the movement speed. In this research, a speed of 70 was used to prepare all the membranes. It is noteworthy that the tensile speed of the polymer solution is also one of the factors that affect the final morphology of the membrane.

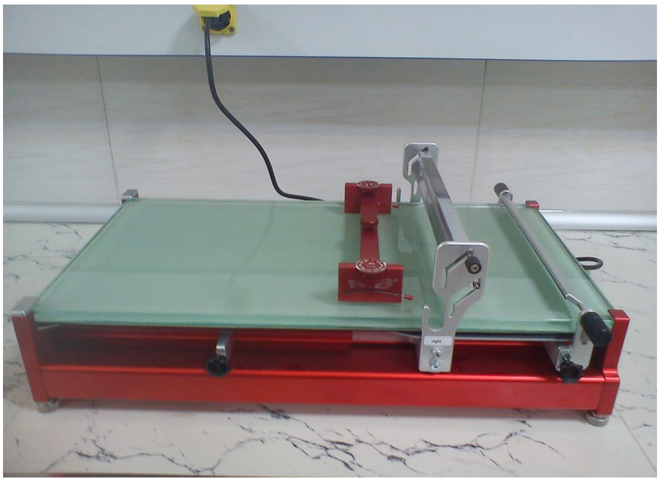

Figure 3: Automatic film maker used in this study.

To smooth and flatten the polymer solution on the glass surface, a film maker with a constant thickness of 200 microns made by the Elcometer Company was considered. Then, at a rapid evaporation time of 15 seconds for all membranes, they were placed in a coagulation bath at a constant temperature of 20°C. After a few seconds, a layer of solid polymer film formed on the glass surface and gradually peeled off. The fabricated membranes were kept in distilled water for two days for complete removal of solvent

In this research, the percentage of polymer, the type of solvent, the type of additive, as well as the temperature conditions of the coagulation bath was investigated on the morphology of the fabricated membranes. Also, 20% polymer in dimethyl acetate solvent and 4% additive were used to make contacting membranes.

Casting membrane with different polymer concentration

In this section, the effect of polyvinylidene fluoride polymer concentration in a solvent and constant coagulation conditions on membrane morphology is investigated. In this experiment, Dimethyl acetamide (DMAc) as a solvent, distilled water as an anti-solvent, and a constant coagulation bath temperature of 20°C, as well as a constant evaporation time of 15 seconds without additive to the polymer solution of the fabricated membranes have been considered.

To investigate this parameter on morphology, polymer solutions consisting of 15-18-21-24-27-30 weight percentages of PVDF polymer in dimethyl acetate (DMAc) were made. Then the membranes were fabricated with fixed conditions and with the steps mentioned in the previous section. The fabricated Membranes were tested by electron microscopy (SEM) for morphological examination. To facilitate the name of membranes, the following codes are consdiered according to Table 3.

Table 3: Following codes of fabricated for polymer solution.

Fabricated membrane code	Solvent	Polymer weight percentage
M15	DMAc	15
M18	DMAc	18
M21	DMAc	21
M24	DMAc	24
M27	DMAc	27
M30	DMAc	30

Casting membrane with different solvents

In this section, the effect of the solvent type on the membranes fabricated from polyvinylidene fluoride (PVDF) polymer is investigated. For this part of study, the three most widely used solvents for PVDF polymers, dimethyl acetamide (DMAc), dimethylformamide (DMF) and normal dimethyl pyrrolidine (NMP) solvents, are considered in a constant condition with a weight percentage of 20% of the polymer and constant temperature and evaporation conditions. Also, no additives were added to the polymer solution. An electron microscope (SEM) was employed to investigate the effect of solvent type on the morphology of fabricated membranes. Table 4 lists the specifications of the fabricated membranes.

Table 4: Lists the specifications of the fabricated membranes.

Fabricated membrane code	Polymer weight percentage	Solvent type
MDMAc	20%	DMAc
MDMF	20%	DMF
MNMP	20%	NMP

Casting membrane with different coagulation bath temperature

At this stage of the experiments, the parameter of coagulation bath temperature on the morphology of the fabricated membranes was investigated. The coagulation bath was used at temperatures of 5-15-25-45-55-65°C. In all cases, the percentage of polymer was constant and equal to 20 wt% and the anti-solvent of pure water was used. The coagulation bath temperature was fixed on the desired temperature using a regular circulating system with high accuracy. Also, in this section, the effect of coagulation bath temperature on two different solvents NMP and DMAc at a constant polymer concentration of 20% was investigated to make the result more accurate. It should be noted that NMP has the highest boiling point, and DMAc has the lowest boiling point among the solvents used. Therefore, two different solvents were used to ensure the trend of changes and the behavior of hydrophobic PVDF polymer to be observed next to two different solvents at different temperatures. Investigations and temperature differences on the structure and morphology of the membrane have been performed using electron microscope images. Table 5 displayes the specifications and codes of each of the manufactured membranes.

Table 5: The specifications and codes of the fabricated membranes.

Fabricated membrane code	coagulation bath temperature	Solvent	Polymer percentage
MN05/MD05	5	NMP/DMAc	20%
MN15/MD15	15	NMP/DMAc	20%
MN25/MD25	25	NMP/DMAc	20%
MN45/MD45	45	NMP/DMAc	20%
MN55/MD55	55	NMP/DMAc	20%
MN65/MD65	65	NMP/DMAc	20%

Casting membrane with different additives

In this section, the effect of different inorganic and organic additives from different families such as: salts, polymers, weak anti-solvents, alcohols and weak secondary solvents (acid), which are lithium chloride (LiCl), polyethylene glycol (PEG 400), methanol and acetic acid were studied on the membrane morphology. The weight percentage of the polymer in each of the fabricated membranes is 20 wt% and the solvent is DMAc. Also, the weight percentage of additive added to the polymer solution is 4 wt%, in each solution the amount of additive was added with respect to the polymer.

Also, an electron microscope test was employed to examine changes in the morphology of the membranes. Table 6 reveals the specifications and codes of each of the fabricated membranes.

Table 6: The specifications and codes of the fabricated membranes.

Fabricated membrane code	Additive (4 wt%	Solvent	Polymer percentage
Mpeg	PEG 400	DMAc	20%
MLic	LiCl	DMAc	20%
MAca	Acetic acide	DMAc	20%
MMet	Methanol	DMAc	20%
MGly	Glycerol	DMAc	20%
Mnon	Non additive	DMAc	20%

CHARACTERIZATION

Phase diagrams

In this project, to investigate the thermodynamic and kinetic aspects of the coagulation process, phase diagrams of polymer solutions were generated at a constant temperature of 20°C in the presence and absence of methanol, polyethylene glycol, acetic acid, lithium chloride and glycerol additives. The method is that instead of drawing a binocular curve, only one binocular point was drawn because, according to previous research, the trend of changes in binocular points is almost constant, so with one point of the binocular diagram, the binocular line can be predicted [44]. Therefore, a polymer solution containing 10 wt% of PVDF in DMAc solvent was prepared for generating a curve without additive, and after 24 hours at a constant temperature, using a burette containing distilled water as an anti-solvent, water was added dropwise to the solution. During the addition of water as a solvent to the polymer solution, for each drop added, the solution moves slightly away from its steady-state and approaches the unstable state. For this reason, with the addition of each drop of water, the polymer solution comes out of a uniform and transparent state and after a while, returns to its uniform and transparent state. But this solution is no longer as stable as before. Because in this case, some water instead of solvent surrounds the polymer chain, this process continued until the solution was no longer colorless and became cloudy. This point, which indicates the formation of a semi-stable region for the polymer solution, is called the cloud point. With the addition of more anti-solvent at this point, this area leads to instability and eventually gel formation. In this research, the observation of this point was done by the naked eye. Figure 4 shows an overview of how to perform the cloud point test.

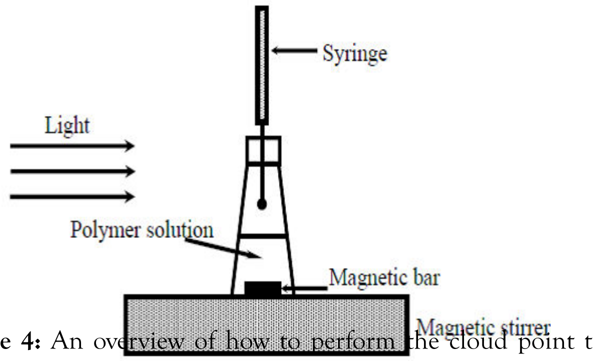

Figure 4: An overview of how to perform the cloud point test [54].

The water anti-solvent strength for the PVDF/DMAc solution was so high that the transparency of the solution changed with increasing one drop of water. It should be noted that in addition to the phenomenon of phase separation, the diffusion phenomenon also plays an important role due to the role of kinetics in controlling the rate of phase separation in the coagulation process and determining the final morphology of the membrane. Then, to determine the binodal points related to the effect of various additives such as polyethylene glycol (PEG), lithium chloride (LiCl), acetic acid, methanol and glycerol, 2 wt % of additive was added to 10 wt% of PVDF polymer solution, and this process continues after homogenization of the solution until a cloud point was obtained, as done previously. It should be noted that all phase diagrams were generated using Sigma plot.12 software.

Scanning electron microscope (SEM)

In order to study and observe the morphology of the formed membranes, a VEGA\TESCAN model electron microscope made in the Czech Republic was used. This microscope was employed to observe the cross-section of the membrane. In order to image the cross-section of the membranes, they were first immersed in liquid nitrogen and then broken in the same medium over time. Also, to generate conductivity in the prepared samples, they were coated with gold metal and after placing in the machine, SEM image was taken from them. These studies were performed at room temperature with magnifications of 1000, 2000 and 5000 times and with a voltage of 20 kV.

Measuring the overall porosity

Another method used to study the morphology of the membrane is to examine the porosity of the membrane. For this purpose, the percentage of overall porosity will be obtained using a method called the gravimetric method as well as the Equation 1.

In this test, the method was that the tested membranes of the same size were prepared first. Each membrane was then immersed at room temperature in a crystallizer containing the organic substance 2-ethyl hexanol and left there for 30 minutes. During this time, the membrane, which was initially white, after half an hour of immersion in a bath of 2-ethyl hexanol, becomes completely colorless and transparent, which indicates the complete penetration of this alcohol in the structure of the membrane? It should be noted that the reason for using this alcohol for porosity testing is its high permeability in the PVDF membrane and its high durability in the environment due to its high boiling point (180-188^{o}C). The percentage of porosity is obtained using Equation [54].

$$\varepsilon = \frac{\frac{m_n}{\rho_n}}{\frac{m_p}{\rho_p} + \frac{m_n}{\rho_n}} \qquad (1)$$

Where $m_n$the weight of absorbed 2-ethyl hexanol is, ρ_n is the density of 2-ethyl hexanol, m_p is the weight of dry membrane, and ρ_p is the density of PVDF.

The weight of absorbed ethyl hexanol is obtained from the difference between the weight of wet and dry membranes.

Measurement of water passing flux

After fabricating the membranes, pure water flux was taken from them in order to study the permeability properties of the solutions. There are generally two ways to perform this test, which are: Cross flow and Dead-end flow

In the cross-flow test, the fluid moves parallel to the membrane surface and some fluid penetrate and passes through the membrane. In this method, impurities pass through the surface and the desired substance passes through the membrane. In the dead-end method, the fluid strikes the surface vertically and penetrates the feed with adjustable pressure. It is said that more clogging occurs in this method.

Here, the dead-end method was used for the samples. In this device, the aqueous solution is located in a tank above the main chamber, which enters the chamber by opening the drain valve. However, due to the small cavities on the surface, pressure must be applied to the solution to allow it to pass through the membrane. Nitrogen gas is used for this purpose because being neutral. This device is equipped with Rs multi-ver software. 1.1w to determine the data. In this test, the membrane with a diameter of 6 cm was placed in an aluminum cell with a polyamide blade (to prevent the membrane from rupturing) and was exposed to nitrogen gas at a pressure of 3 bar for 90 minutes. The schematic of the device is shown in Figure 5.

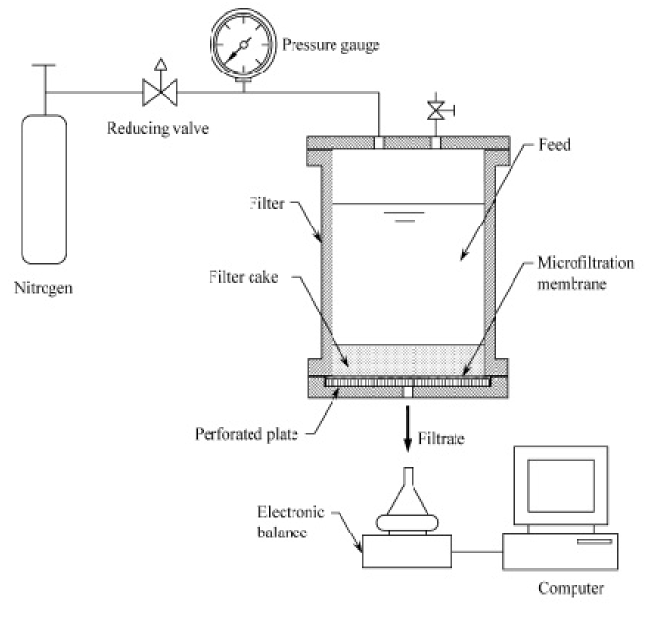

Figure 5: The schematic of the device [55].

This test was performed only to investigate the effect of the additive on the amount of pure water flux passing through the membrane and to study the additive effect on the hydrophilicity of the membrane. The higher the hydrophilicity of the membrane and the porosity of the membrane, the higher the output water flux.

Gas permeation test (GPT

In this test, nitrogen gas passing through a high precision regulator (0-4 bar) is used to adjust the inlet pressure of the flat membrane module, which has a closed retentate flow and open permeate flow.

The flow rate is measured by a mass flow meter in the high flow range and a bubble flow meter in the low flow range, depending on the polymer concentration and the structure and morphology of the fabricated membrane [56]. Fig. 6 shows the schematic gas permeation test setup.

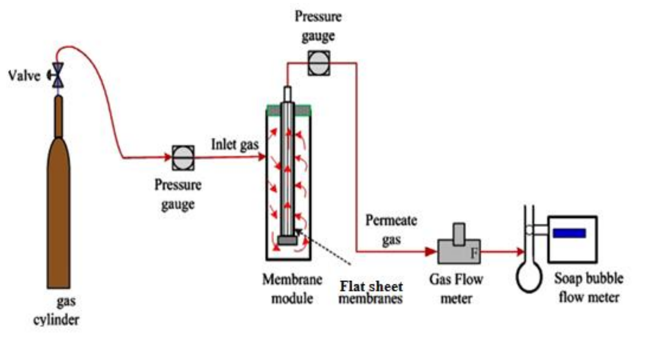

Figure 6: The schematic of gas permeation test setup for measuring pore size and surface porosity [56].

Pore size and membrane surface porosity calculation

The required equations to calculate the average pore size and effective membrane porosity are presented in this section. It is assumed that the cavities are cylindrical around the surface, which is a valid assumption according to the surface SEM images in Equation 2 [7].

$$J=\frac{2}{3}\left(\frac{8RT}{\pi M}\right)^{0.5}\left(\frac{r_p}{RT}\right)\left(\frac{\varepsilon}{L_p}\right)+\frac{1}{8\mu}\left(\frac{{r_p}^2}{RT}\right)\frac{\varepsilon}{L_p}P_{av} \qquad (2)$$

As mentioned earlier, the first term of this equation shows the influence of Knudsen diffusion and the second term shows the influence of Poiseuille diffusion. The parameters of this equation can be described as follows:

J: Outlet gas flow flux from flat membrane module (mol/ m^2.s.pa)

r_p: radius of membrane pores (m)

L_p: length of effective pores in membrane structure (m)

Ɛ: Membrane surface porosity

R: Global gas constant, 8.314 (J/mol.K)

μ: Viscosity of input gas (nitrogen) (kg/m.s)

M: Molecular weight of inlet gas (kg/mol)

T: Inlet gas temperature (K)

P: Arithmetic mean pressure between the pressure of inlet and outlet gas flow (Pa)

In this experiment, the pressure is regularly increased 0.3 bar by the regulator, and after each pressure increment, the amount of permeate flow is measured by a bubble flow meter. By plotting the J value in terms of the average pressure difference between inlet and outlet nitrogen flow (atmospheric pressure) and obtaining first-order fitting function from these points, the average pores size and effective porosity of the surface can be achieved as follows [1]:

A= fitted line width of the origin

B= fitted line slope, then

$$J=A+B^{*}P_{av} \qquad (3)$$

$$J=r_p=5/333\frac{B}{A}\left(\frac{8RT}{\pi M}\right)^{0/5}\mu \qquad (4)$$

$$\frac{\varepsilon}{L_P}=\frac{8\mu RTB}{{r_p}^2}$$

Measurement of inlet liquid critical pressure

This device is designed to measure the maximum size of the pores as well as the minimum pressure for the liquid to enter the membrane. The smaller the pore size, the more pressure the liquid flow must have to penetrate, so the minimum pressure will be higher.

The following items are used in this experiment setup; a flat membrane module, a reservoir for the inlet fluid, a nitrogen gas capsule, and a regulator for applying pressure on the liquid inside the reservoir. The pressure increases slightly on the liquid and it enters the membrane cell. After each increase of pressure (about 0.3 bar), half an hour is given to see if the liquid comes out. Finally, due to the increase of pressure on the liquid entering the module, it suddenly passes through the tube in a specific pressure called critical pressure. Then, the maximum size of the pores can be obtained by the following equation [57].

$$\Delta P=\frac{2\delta COS\theta}{r_p} \qquad (5)$$

In this Equation (5), δ is the water surface tension (72.8×10-3 N/m), θ is the contact angle between water and the membrane surface, which is usually 0 degrees for the first drop to exit, rp is the maximum pore through which water passes, and ΔP is the critical pressure of the fluid entering the membrane [55]. Fig. 7 determines the schematic of this device.

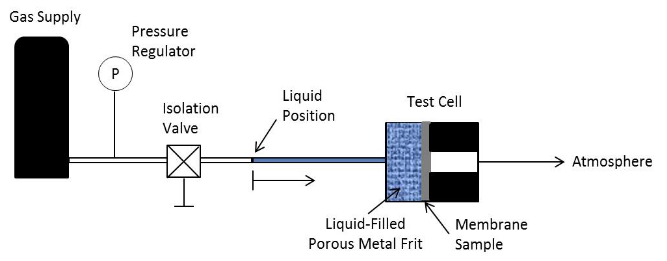

Figure 7: Schematic of experiment setup for measuring critical pressure of inlet liquid [55].

RESULT AND DISCUSSION

Investigating the effects of solvent type on membrane structure

As mentioned in the section regarding the mechanism of membrane formation , if the solvent and anti-solvent have a high degree of miscibility and reciprocity, the penetration of the solvent into the film and the exit of the solvent in the opposite direction (into the setting containing anti-solvent) will be accelerated. Indeed, the speed of this phenomenon depends on two important parameters, namely thermodynamics and kinetics, and it is the competition between these two indicators that stabilize the morphology of the membrane. Obviously, increasing the phase separation rate increase the enrichment of the film with anti-solvent and thus leads to the formation of membranes with higher porosity and vice versa. The degree of miscibility and solubility of both solvent and anti-solvent has a direct relationship with the similarity between their molecular structures. Figure 7 shows the electron microscope results of membranes made with DMAc, NMP and DMF solvents. The results are related to the fabrication of membranes with 20% by weight of the polymer and in equal coagulation conditions without any specific additives.

Since the coagulation setting is water for all solvents, which has polar molecules, it is necessary to use polar solvents such as normal methyl pyrrolidine (NMP), dimethyl Acetamide (DMAc) and dimethylformamide (DMF) for better mixing between solvent and anti-solvent, which obviously results in an increase in the porosity of the resulting membranes. However, the use of non-polar solvents such as acetone, tetrahydrofuran, etc., due to the immiscibility with water, slows down the transfer rate of solvent and anti-solvent during membrane formation. Therefore, it delays the enrichment of the film with anti-solvent and leads to a non-porous morphology.

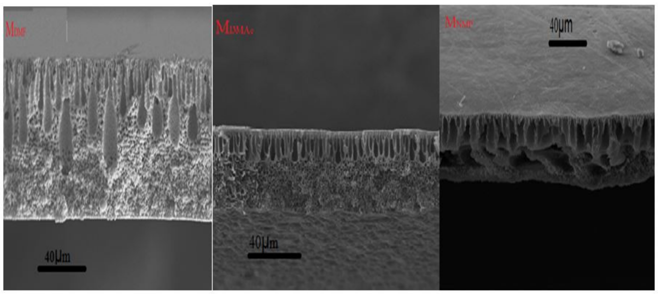

Figure 7: Electron microscope images show the effect of solvent type on the morphology of fabricated membranes (M DMAc-MNMP MDMF).

Also, according to the Manori, et al. [5], the binocular diagram 8 can be drawn for PVDF polymer using different solvents, as can be seen in the order of phase separation for NMP<DMF<DMAc solvents, i.e., the phase separation process is performed faster in NMP solvent, which indicates that the viscosity of the solutions made with NMP solvent is lower than DMF and DMAc, so fast phase separation occurs.

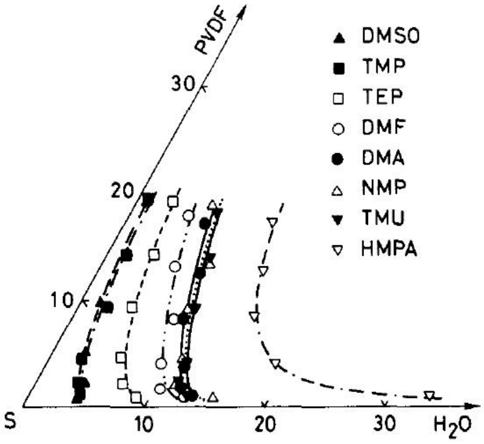

Figure 8: Binocular diagram can be drawn for PVDF polymer using different solvents [5].

Furthermore, according to Hansen parameters, which are defined for the amount of solubility of the polymer in solvent and anti-solvent, as well as the solubility of solvent and anti-solvent in each other, so the solubility was also examined by this method. Table 7 illustrates the Hansen parameters for solvent, anti-solvent and polymer [58].

According to this table, δ_d is a parameter related to the breaking force between molecules, δ_p is a parameter related to polar forces, and finally, δ_h is a parameter related to hydrogen forces between molecules, which according to Equation 6, $\Delta\delta_{ps}$ and $\Delta\delta$ S_{sn} is obtained. In the above notation, S stands for solvent, P stands for polymer and n stands for solvent.

^{a} The data is calculated from the repeating unit of the polymer $\delta_t = \sqrt{\delta_d^2 + \delta_p^2 + \delta_h^2}$

Table 7: Hansen parameters for solvent, anti-solvent and polymer.

Chemicals	δd	δp	δh	Molar Volume	δta	Δδps	Δδsn
PVDF	17	12.1	10.2	-	23.22	0.632	-
DMAC	16.8	11.5	10.2	92.5	22.77	3.168	32.48
NMP	18	12.3	7.2	96.5	22.95	1.982	35.38
DMF	17.4	13.7	11.3	77	24.86	-	31.14
Water	15.5	16	42.3	18	47.8	-	-

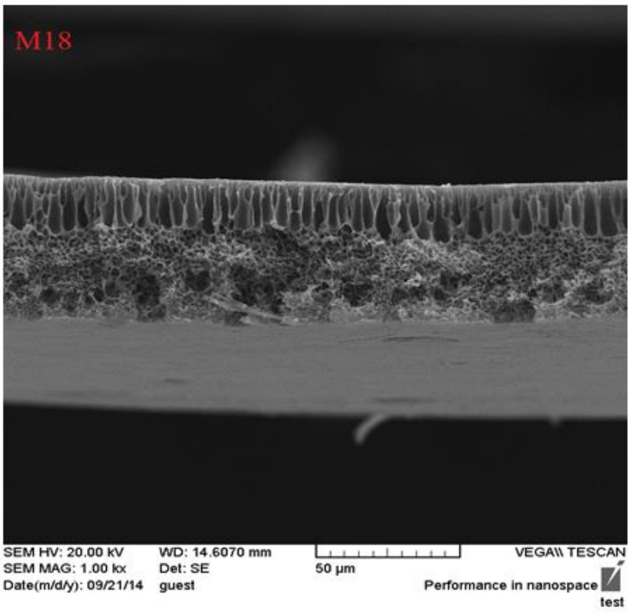

According to the studies [20, 31, 59], between the two parameters Δδps and Δδsn, the solubility parameter between solvent and anti-solvent is more important than the parameter between solvent and polymer. According to the data in this table, it can be seen that there is the largest difference between Δδsn of water and NMP, so it has the highest solubility and has a higher phase separation rate, so the morphology has moved towards macro-cavity. Also, the tear cavities between water and DMF, and finger cavities between the water and DMAc will be shaped. In fact, the greater the Hansen difference between solvent and anti-solvent, the greater the miscibility, the faster the phase separation, and the more porous the macro structure. According to these data, it can be claimed that the greater the difference in solubility parameter between the polymer and the solvent, the higher the expectation of macro-cavity structural. Electron microscope images show the effect of solvent type on the morphology of fabricated membranes in Figure 7.

In general, the chemical structure between solvent and anti-solvent is very important. If it is necessary to form membranes with smaller pore size and more porosity, the degree of miscibility and solubility of solvent and anti-solvent has a direct relationship with the similarity between their molecular structures. For example, if non-polar organic liquids are used for anti-solvent, if polar solvents are used, the phase separation process will be slow, and the structure will be dense. If non-polar solvents are used, the phase separation process will be fast, and the structure will be porous. Therefore, if the anti-solvent is polar, polar solvent is required for the porous morphology, and for a dense morphology, a non-polar solvent is required.

Investigating the effect of polymer concentration

In this section, the effect of polymer concentration on membrane morphology is investigated. As mentioned in the previous section, solutions with concentrations of 15-18-21-24-27-30% by weight of polymer with dimethyl acetate solvent (DMAc) with the same preparation conditions were formed into a flat membrane. Then, the dried membranes were prepared for electron microscopy examination for morphology and structure. Figure 9 presents the results of the SEM test with the codes described in the previous section.

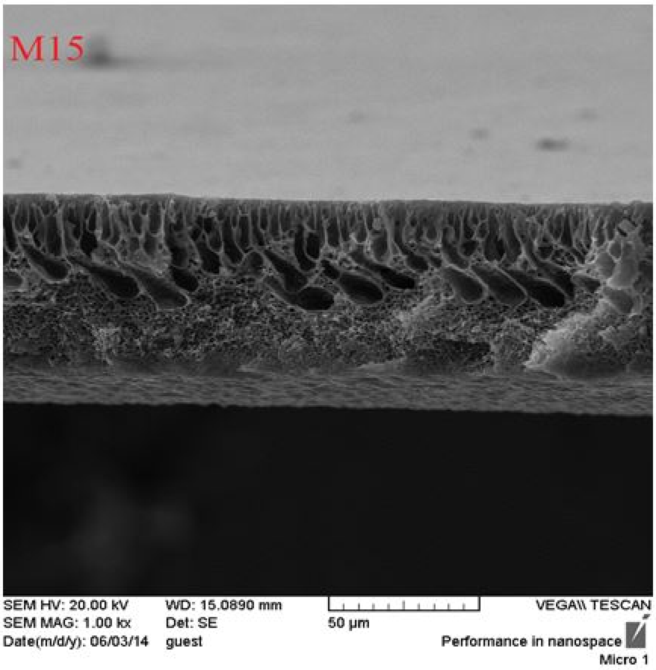

Figure 9: The results of the SEM test with the codes described.

As it can be seen, the membrane structure changes from tear cavities at low concentrations to regular finger cavities at medium concentrations and the higher the concentration, the more regular the finger cavities are placed next to each other. Finally, at concentrations above 30% by weight of the dense structure polymer, at some points, macro is formed due to the entrapment of water-solvent in the inner structure of the membrane due to the so-called hardening of the skin layer and the entrapment of these droplets of anti-solvent into strong polymer chains that remain inside the membrane and create cavities [60]. Increasing the concentration of polymer in the polymer solution means increasing the density and compactness of the polymer chains. Obviously, in this case, due to the high compaction of the polymers in the initial state solution, the space required to move the polymer chains away from the solvent-rich nuclei will be limited due to the lack of space (phase separation rate slows down). Because the regression and accumulation of polymers around the antifouling locations require the presence of space, which is practically limited in the case of initial accumulation of polymers due to the high initial concentration of polymer in solution. Now, the higher the polymer concentration, the less space there will be for the polymer chains to move and the faster the nuclei will stop growing. In fact, the phase separation process will be slower. It can be clearly seen in the phase separation process with the naked eye in the coagulation bath, which means that it takes longer for the membrane to separate from the glass, resulting in smaller final cores and smaller pores and membranes with more porosity are created.

On the other hand, with increasing the weight fraction of the polymer, the viscosity of the polymer solution increases, and it is obvious that in this case, the mobility of the film and all its components, including the growth of solvent-rich and anti-solvent cores will be slowed down, which can create a membrane with a dense structure. In fact, limiting the growth of solvent-rich and anti-solvent cores provides an opportunity for anti-solvent penetration from other surface areas of the film, resulting in new nuclei next to the old cores (i.e., in some points, anti-solvent penetrates quickly, usually near the surface, and in some points, it penetrates slowly). As a result, the nuclei do not grow harmoniously with each other and the membrane structure is seen as densely heterogeneous. If there are cavities, the cavities grow heterogeneously, as it showed in the 30% PVDF polymer in M30. As a result, the growth of a limited number of nuclei will be prevented and the growth will be divided among more of them, which in turn can lead to the formation of more nuclei with smaller sizes and, consequently, a denser membrane structure. Generally, increasing the percentage of polymer increases the density of polymer chains and consequently increases the intermolecular gravitational force for polymer chains, which increases the force for coagulation since the tendency of solvent and polymer has decreased due to increasing concentration. Therefore, the decrease in coagulation rate due to the increase in concentration depends on the balance of the two mentioned forces.

Investigating the effect of coagulation temperature

In general, it is thought that by decreasing the coagulation temperature due to the slowing of the phase separation process, a membrane with more porosity and smaller pore size is obtained, and with increasing temperature due to the faster phase separation process, the membrane morphology should move towards macro cavity structure with the less porosity, and vice versa in some cases. The type of polymer is very decisive on how the membrane is formed so that for polyethersulfone polymer, the porous structure will be created with increasing temperature and with the decrease in coagulation temperature, a dense structure will be created. But for PVDF polymer, the opposite happens, which is one of the factors of hydrophobia of this type of polymer [28, 50]. In this research, for the weight percentage of 20% polymer solution made of PVDF polymer, with increasing temperature, the structure progressed to a dense membrane, and conversely, with decreasing temperature, coagulation of the structure became pore-like, as clearly shown in Figure 10 from electron microscope images. In these figures, according to the coding mentioned in the previous section, the temperature of the coagulation is 5-15-25-45-55-65°C. Also, two solvents, dimethyl acetamide (DMAc) and normal methyl pyrrolidine (NMP) were used to evaluate the effect of solvent and temperature to mention the results with more certainty (DMAc has the lowest boiling point and NMP has the highest boiling point). The polymer concentration was kept constant at 20% by weight in all experiments.

It can be seen clearly that, with increasing temperature, the density between the polymer chains decreases and consequently, the intermolecular attraction force for the polymer chains decreases, which increases the reaction force for the phase separation phenomenon and increases the phase separation rate. PVDF polymer may behave differently from other polymers and except for the hydrophobicity of this polymer, with increasing temperature, the speed of solvent exit from the polymer solution increases compared to the speed of anti-solvent entry into the polymer solution and may enter the Jellies and crystals structure region according to three-phase diagrams. So, it is obvious that the structure will condense as the temperature increases, as electron microscope images confirm, and as the temperature decreases, the exact opposite will happen and the structure will move toward the macro cavity [53,54]. Figure 10 reports how the membrane formation happened in the experiments.

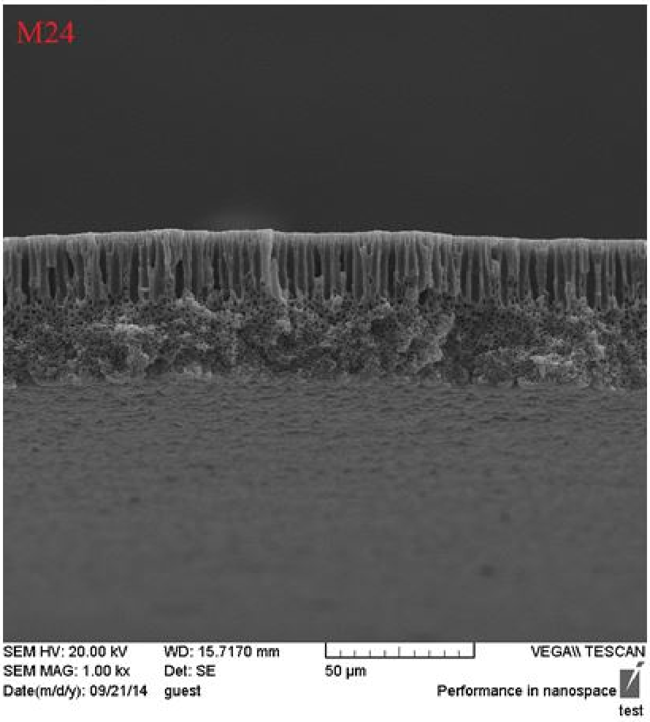

Figure 10: Effect of coagulation temperature, electron microscope images.

In further explanation of this process, it should be said that by decreasing the temperature, the velocity of the solvent leaving the polymer solution and the velocity of the anti-solvent entering the polymer solution is equal (Path 3 in the figure above) and according to the phase diagrams, the interface line of the membrane formation does enter the quasi-stable region and directly enters the unstable region. Therefore, it undergoes spinodal decomposition and turns into two phases rich in polymer that forms dense and poor points of polymer that form cavities. However, these two phases is constant and the composition of their percentage and cavities is constant and is determined by the interface lines. Therefore, at low temperatures, it occurs in the case of PVDF polymer, which is called spinodal decomposition and ultimately leads to a macro structure. In this case, none of the rich and poor nuclei of the polymer are controlling the reactions. When the temperature increases, the solvent and anti-solvent displacements also increase. As a result, because the solvent exits faster than the anti-solvent, with the solvent leaving, the polymer chains find each other and become separated when the anti-solvent enters. However, at high temperatures, the solvent exits faster than the anti-solvent, so the dense structure will form faster, and at high temperatures, the interface line may not enter the unstable region at all and enter the jelly state directly (path 1 in the figure above), creating a completely dense structure.

Examining the phase diagrams to investigate the effect of temperature, Figure 11 shows that with increasing temperature, the binodal curve moves to the right, i.e. the polymer-antisolvent axis, which means that the thermodynamic stability increases with increasing temperature. On the other hand, kinetics also increases, but the competition between these two parameters determines the final structure of the membrane.

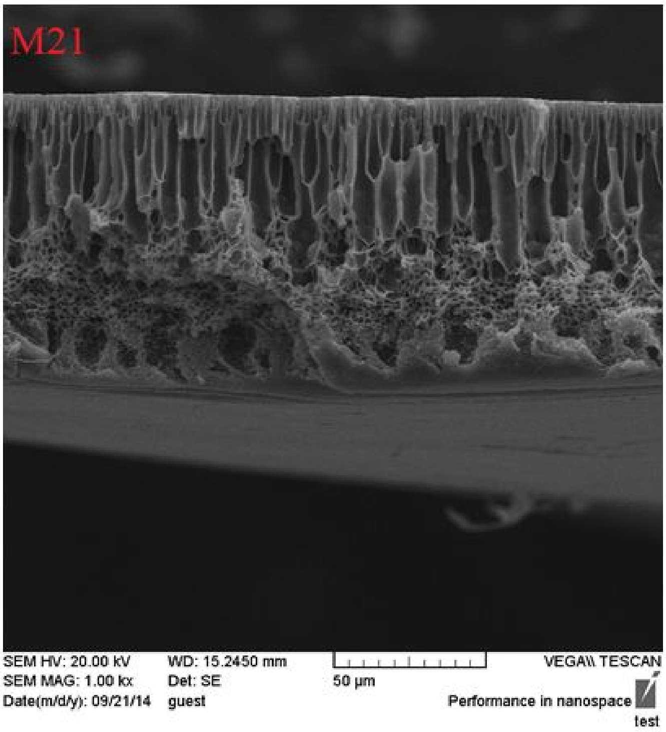

Figure 11: Shows that with increasing temperature, the binodal curve moves [12].

As the temperature increases, the power of DMAc decreases. Previous studies have shown that the DMAc solvent weakens with increasing solution temperature, i.e., the random coil becomes smaller. This is due to the increased resonance of the DMAc solvent with temperature and thus the effect of the DMAc solvent on the C-F of the PVDF chain.

However, with increasing temperature, the effect of entropy is greater than decreasing the solvent strength and causes the binodal boundary line to be inclined towards the polymer-anti-solvent axis. Therefore, with increasing temperature, this diagram moves towards the polymer-anti-solvent axis. The phase diagram examines the kinetics and thermodynamics governing the membrane, so moving the binodal to the right means that increasing and decreasing the temperature will have a significant effect on the thermodynamics and kinetics of the membrane. Therefore, the final structure of the membrane is determined by the dominance of one of these two parameters over the other. In fact, when the binodal goes to the right axis, according to studies, the kinetic power decreases and the thermodynamic effect increases, and the binocular movement to the left indicates that the kinetic power is high and the thermodynamic effect decreases [12]. Figure 12 shows that effect of temperature on bimodal curve moves.

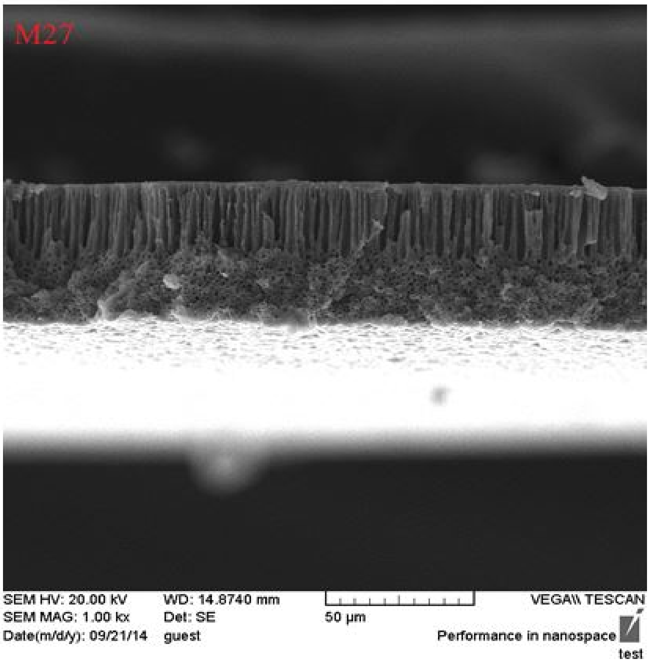

Figure 12: Shows that effect of increasing temperature on the binodal curve moves [12].

By observing the SEM image, it is clear that the temperature range of 20-25 °C, due to the regularity in the elongation of the cavities, can have the desired structure for optimal performance in membrane contactors, so that different researchers in the field of membranes contactors choose this temperature range as the temperature of the coagulation [28,46-47]. Accordingly, the coagulation temperature for the membranes of the performance analysis section of this research is considered to be 20 °C.

Investigating the effect of various additives on morphology

The cavities of a membrane (both surface cavities and cavities in the membrane body) are generally the pathways of the components (additive or solvent) through it, and therefore the presence of these cavities in the membrane morphology is very important. An increase in their number, depending on the type of membrane application, increases the amount of product passed in a certain period of time. One of the most important results of using some types of additives in the initial composition of polymer solutions is the formation of membrane cavities due to their presence. Therefore, sometimes the purpose of adding an additive is to actually form cavities in the membrane morphology. The additive can also be used to change the intensity of hydrophobicity and hydrophilicity. It should be noted that the role of additives in this approach is that their presence areas as a suitable place for anti-solvent penetration and thus the rejection of the polymer is considered, which results in a hole in the surface of the membranes. Accordingly, it is necessary that the miscibility between the polymer and the additive be low so that the polymer can easily reject the additives and cavities can form. Therefore, the lower the miscibility, the larger the pore size [12].

In Figure 13, five types of additives from different groups such as polyethylene glycol from the group of polymeric additives, lithium chloride from the group of organic salts, methanol from the group of alcohols, acetic acid from the group of weak acids, and glycerol from the group of anti-solvents with 4 wt% relative to the amount of polymer in solution, were used respectively, at a constant polymer concentration of 20 wt% and dimethyl acetate solvent with equal coagulation conditions. The differences are clearly visible since the images are taken in two cases with different magnification percentages from the cross-section and the top layer of the membrane.

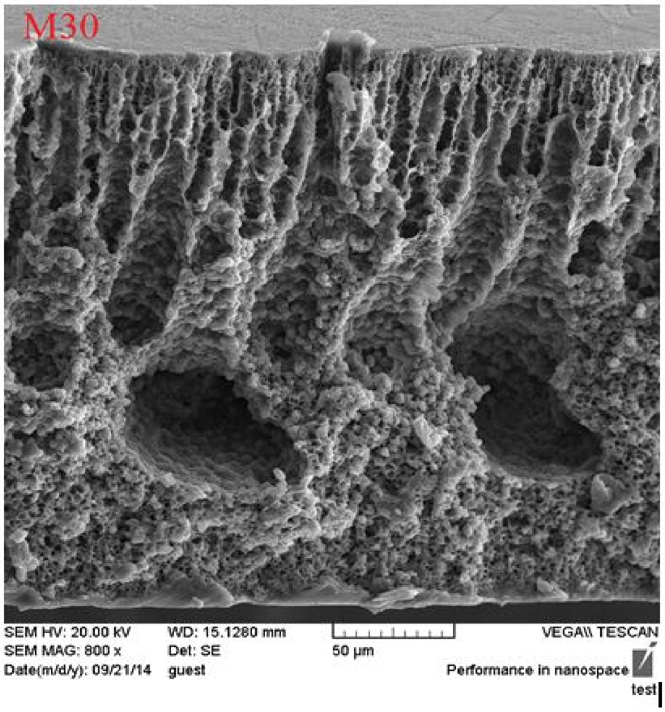

Figure 13: SEM images related to the effect of adding different additives to the polymer solution: The left image shows the membrane cross-section and the right image shows the upper layer of the membrane.

As it can be seen, the cavities are created using the additives, which are because of being rejected by the polymer chains due to the low miscibility between the polymer and the additive and the high miscibility between the anti-solvent and the additive. Therefore, the additives push away the polymer around the film and forms surface cavities. Then, by penetrating deep into the film structure, other polymers in its path are also rejected around, thus forming small cavities and high porosity in the thickness of the membrane. Due to the above experiments, it is expected that by increasing the concentration of additive, more cavities will be created on the surface of the membrane, and more paths will be created for the anti-solvent to pass into the polymer, so the membrane structure will be more porous. As the concentration of the additive increases, the viscosity of the solution also increases, which has a significant effect on the phenomenon of phase separation and slows down the separation process. In fact, as mentioned, the two parameters of thermodynamics and kinetics are very important in the final morphology of the membrane. In this case, the addition of various additives reduces the thermodynamic stability, but the viscosity of the solution increases, thus reducing the phase separation kinetics, and the superiority of each of these two parameters determines the final morphology of the membrane. In fact, with decreasing the stability of the structure, the membrane becomes porous and with increasing viscosity, the morphology moves towards compaction. So, to create a cavity inside the membrane, we have an optimal point for adding different additives. From that point on, it is the viscosity of the solution that determines, and the structure will move toward compaction instead of porosity. Figure 14 clearly mentions that the effect of the additive on the binodal curve that with the addition of the additive the curve moves to the left, i.e. the polymer-solvent line, which means that the thermodynamic stability will decrease.

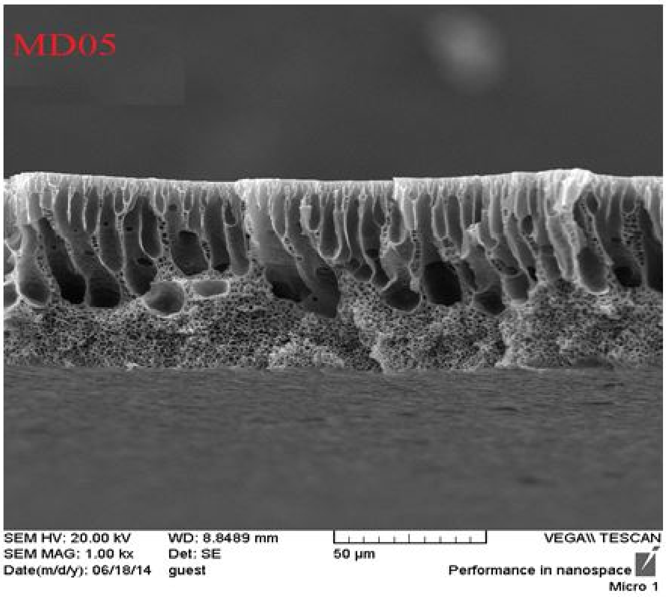

Figure 14: The effect of the additive on the binodal curve that with the addition of the additive the curve moves [54].

In order to have a better investigation of the additive effect and its role on the thermodynamics and kinetics of the membrane, phase diagrams and its effect on the binodal diagram are investigated.

The effect of additive on the thermodynamics and kinetics of the polymer solution is investigated by cloud point experiment and diagram drawing.

As explained in the previous section, the binodal point was obtained using the cloud point method for the solution by combining 10 wt% of the polymer and 4% of the additive.

Of course, it is necessary to mention this point, because the motion of the binodal line is fixed in different sources, so in this research, it was enough to take only one point of the binodal line path, and with one point, the approximate path of the binodal curve can be assumed. Figure 15 displays the result of the work to draw a binodal point.

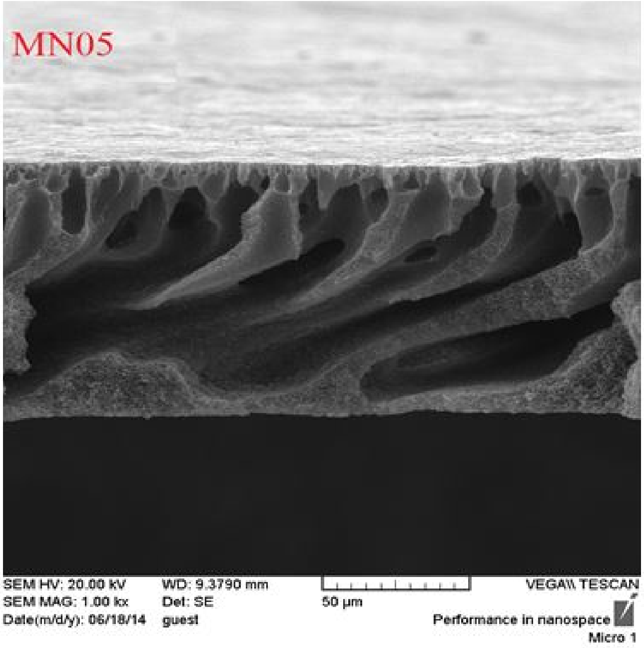

Figure 15: Phase diagram for membrane solution PEG (◙), Acetic acid (◙), Methanol (◙), Glycerol (◙), LiCl (◙) and Pure PVDF (◙).

As it can be seen, with the increase of additive, the binodal line moves towards the polymer-solvent curve, which means more instability. In fact, according to the phase diagram zoning described in the first section, as shown in Figure 17, the length of the stability zone decreases and consequently, the thermodynamic stability decreases. Therefore, with the least amount of anti-solvent, it quickly enters the quasi-stable region and enters the spinodal decomposition and forms two rich and lean phases of the polymer. On the other hand, with adding additives, depending on their type, the viscosity increases and affects the kinetics, so adding the additive reduces the thermodynamic stability and increases the viscosity of the solution. All these factors cause the formation of porosity in the membrane. The type of additive, polymer, solvent, and other parameters will determine the length of the pores and the amount of surface porosity.

According to the above explanations, the presence of additives with anti-solvent properties has two simultaneous opposite effects on the morphology of the resulting membrane. On the other hand, due to the intensification of thermodynamic instability and the creation of cavities in the surface of the film in phase separation, the basis for increasing the rate of enrichment of the film with solvent, which facilitates the formation of membranes with higher porosity and smaller cavities, will be provided. Also, by increasing the viscosity, the transfer of solvent to anti-solvent and the growth of nuclei rich in these two substances during the formation of the membrane becomes difficult, which results in a decrease in porosity and an increase in the size of membrane cavities. Therefore, it can be concluded that the presence of additive can lead to both a more porous morphology and a membrane with a lower porosity morphology, which in turn depends on the formation of membrane motion in phase diagrams and phase separation conditions. Thus, the structure of the membrane depends on which of the two effects ultimately overcomes the other. According to several papers on the study of membrane morphology [31,59] as well as the results of Fauzi Ismail and Matsura on membrane contactors [56,61-63], if thermodynamic dominates, the morphology becomes porous and if the viscosity (kinetics) dominates, the morphology becomes dense.

Based on the phase diagram 15, it can be seen that polyethylene glycol has the binodal point closest to the polymer-solvent axis, so it seems that it should have the highest thermodynamic instability and should have a completely porous structure with small holes compared to other additives, however, it is not.

Here is the solubility kinetics that plays a role, and the addition of polyethylene glycol leads to an unconventional increase in the viscosity of the solution.

Because polyethylene glycol has a higher molecular weight than other additives and reduces the phase separation kinetics, so the structure is more compact than other additives, which means that the porosity is less, and the size of the cavities is larger. For additives with low molecular weight, such as acetic acid and methanol, binodal has the longest distance from the polymer-solvent axis and the phase separation process is fast, so it has the least instability and must have a more porous structure than other additives. It also has smaller cavities that electron microscope images also show the subject.

Because the porosity and the size of the pores are very important for the contacting membranes, and currently there is no suitable vision to choose the right type of additive for optimal performance in the contacting membrane, the pore size and porosity tests on the additive effect on the membranes should be performed along with the results specified from other parts such as polymer percentage (20 wt%), coagulation bath temperature (20°C) as well as the solvent type (DMAc).

Investigating the additive effect on overall porosity, contact angle

In this section, after examining and fully understanding the morphology of membranes made of polyvinylidene fluoride polymer and analyzing the membrane morphology changes by adding an additive, the effects of additives on the porosity and pore size, etc. of the membranes made for membrane contactors have been investigated.

The weight percentage of the polymer for making the initial membrane is 20%, the coagulation bath temperature is 20°C, and the solvent type is DMAc.

From each of the mentioned additives, 4 wt% with respect to polymer was added to the polymer solution. Based on the description in section 3, the flat membrane was fabricated, and the following tests were performed.

The additive effect on the three tests introduced in the previous section, which are the overall porosity, contact angle and tensile (mechanical strength) of the fabricated membranes, was investigated.

Table 8: The results of the contact angle, overall porosity and tensile tests.

Membrane code	Additive	Overall porosity	Contact angle (deg)	Tensile (MPa)
M_{Pure}	Without additive	0.52	89.88	7.56
M_{LiCl}	4 wt% lithium chloride	0.64	64.73	8.5
M_{Acid}	4 wt% acetic acid	810	67.83	8.98
$M_{Methanol}$	4 wt% methanol	0.74	65.82	8.05
M_{PEG}	4 wt% ethylene glycol	54	45.74	10.54
$M_{Glyserol}$	4 wt% glycerol	60	0.5378	9.65

The results of the tensile test (mechanical strength) from Table 8 showed that with increasing additive, as the viscosity of the solution increases and the process of phase separation of the membrane formation is slowed down, most of the membrane structure is spongy, so the mechanical strength of manufactured membranes is higher than without additives. Adding an additive to the dense layer of the membrane increases the porosity and the size of the cavities, which increases the tensile strength of the fabricated membranes, so they are more resistant to the tensile test. It is noteworthy that between the above additives, glycerol and polyethylene glycol cause the highest increase in viscosity in the polymer solution, so they have the highest amount of pressure for the tensile test. It can also be seen that with increasing additive, the contact angle decreases because the porosity increases and the movement of water into the structure becomes easier. As Table 8 shows, the larger the contact angle, the greater the porosity of the membrane surface since the pore size is smaller [64]. The acetic acid additive has the highest degree of hydrophobicity, so it should have the most porosity on the surface and have smaller cavities. For polyethylene glycol, due to the high hydrophilicity of this polymer and the fact that the phase separation is slow, so it has less porosity and larger pore size, SEM images can show these changes to some extent.

Investigation of the effect of additive on pure water flux and critical pressure of water entering the membrane

In this section, the effect of additives on the two tests of pure water flux passing through the membrane and the critical pressure of the water entering the membrane is investigated. Obviously, these two tests indicate the degree of hydrophilicity, membrane porosity and maximum cavity in the membrane structure, respectively.

Table 9: The result of critical pressure of input water (psi).

Membrane code	Additive	Critical pressure of input water (psi)
M_{Pure}	Without additive	30
M_{LiCl}	4 wt% lithium chloride	40
M_{Acid}	4 wt% acetic acid	37
$M_{Methanol}$	4 wt% methanol	35
M_{PEG}	4 wt% ethylene glycol	48
$M_{Glyserol}$	4 wt% glycerol	45

According to Table 9, the critical pressure of the inlet fluid increases with increasing viscosity of the polymer solution because the high viscosity helps to form dense structures.

Among the additives, polyethylene glycol and glycerol have the highest viscosity and the critical pressure of the inlet fluid has also increased. The higher the critical pressure, the smaller the membrane pores and the more pressure the liquid needs to pass through the porosity of the membrane, or in other words, the denser the membrane structure and the smaller the pores.

From the critical pressure events and the Laplace relationship introduced in the previous section, the maximum hole size according to Table 10 can be obtained to some extent with a percentage of error.

Table 10: The result of maximum hole size in the membrane.

Membrane code	Additive	Maximum hole size (μm)
M_{Pure}	Without additive	0.713
M_{LiCl}	4 wt% lithium chloride	0.535
M_{Acid}	4 wt% acetic acid	0.578
$M_{Methanol}$	4 wt% methanol	0.615
M_{PEG}	4 wt% ethylene glycol	0.445
$M_{Glyserol}$	4 wt% glycerol	0.475

After the morphology of the membranes was examined by the above tests, its performance was also evaluated.

In this test, the permeability of pure water to membranes was measured. As shown in Figure 16, all membranes initially show a flux that has declined over time.

This downward trend can be attributed to the increased cake (concentration polarization) on the membrane surface. For this reason, over time, due to the presence of cake on the membrane, the flux decreases while the thickness of the cake increases.

It should be noted that in the definition of a cake is known as anything that is placed on the membrane and it can be collected.

However, finally, with increasing the thickness of the cake, the phenomenon of clogging is observed.

As shown in the figure, the flux passing through the membrane containing the lithium chloride additive was greater than the other additive membranes for 90 minutes.

This is due to the different morphology of this type of membrane.

In fact, this issue goes back to the degree of hydrophilicity and hydrophobicity of the membrane and the surface porosity, so that according to Table .

8, the membrane containing lithium chloride has the highest overall porosity and the lowest contact angle, which means that it has the highest hydrophilicity compared to other membranes.

Therefore, from the pure water flux test, it can be concluded that with the increase of different additives, depending on the type of additive, the membrane morphology has improved towards the hydrophilicity, so the water permeability will be higher, as shown in Figure 16.

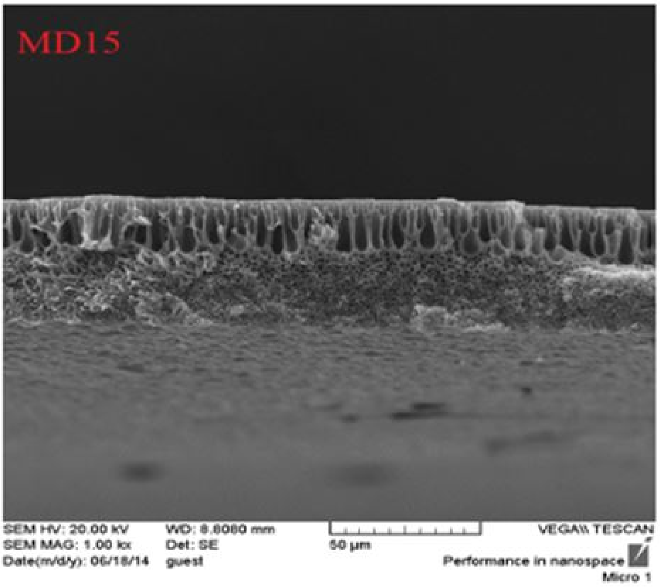

Figure 16: Membrane morphology has improved towards the hydrophilicity, so the water permeability will be higher.

Also, for hydrophilic membrane contactors, hydrophilicity is considered as a negative parameter. Accordingly, from the pure water flux test, it can be concluded that acetic acid additive has a low amount of hydrophilicity, which was also seen in the contact angle results.

Investigation of the effect of additive on effective porosity, surface pore size, and nitrogen diffusion (GPU)

As explained in the previous section, after fabricating membranes with additives such as glycerol, polyethylene glycol, lithium chloride, methanol, acetic acid using the mentioned relations related to the gas penetration test in the third section and using the gas permeability tests device, the surface porosity and average pore size and nitrogen permeation tests were taken from the fabricated membranes, the results of which are as follows.

Figure 17 shows an example of a gas permeability test diagram for pure PVDF. The same is done for the other additives. From the slope and width of the origin of each diagram, the effective porosity of the surface and the average size of the cavities can be obtained, respectively.

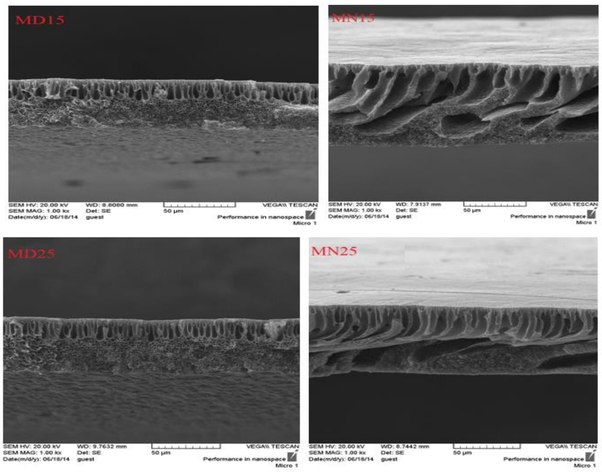

Figure 17: Gas permeability test diagram for pure PVDF.

Finally, after drawing all the figures, the data were recorded in a Table 11, it should be noted that these three parameters are among the most important characteristics of a membrane to have high efficiency in contactors.

Based on these data, the relationship between the effective surface porosity and the average pore size is an inverse relationship, so that with increasing membrane porosity, the surface pore size decreases, but there is no exact relationship for nitrogen penetration testing, and certainly, there are other parameters that affect the rate of nitrogen penetration.

Table 11: Relationship between the effective surface porosity and the average pore size.

Membrane code	additive	Average pore size (nm)	Surface porosity (1/m)	N_2 Permeance at 1*105 Pa(10-5.cm^3/cm.Hg.s.cm^2)
M_{Pure}	Without additive	102	83.671	8.9913
M_{LiCl}	4 wt% lithium chloride	54	554.764	10.918
M_{Acid}	4 wt% acetic acid	37	1123.34	16.654
$M_{Methanol}$	4 wt% methanol	24	987.54	12.765
M_{PEG}	4 wt% ethylene glycol	76	236.656	9.74
$M_{Glyserol}$	4 wt% glycerol	43	754.879	8.7648

The nitrogen penetration test actually shows the amount of nitrogen passing through the membrane under operating conditions for a pressure of 1 bar, which is the same as the GPU for the membrane performance in gas separation. The higher the GPU value, the greater the distance between the polymer chains, which indicates that the membrane shows less resistance to gas permeation. Thus, the membrane permeability increases and the value of selectivity decreases, so there is a competition between GPU and selectivity.

On the other hand, the higher the porosity, the higher the nitrogen permeability, as is the case for acetic acid, which has the highest efficiency (nitrogen penetration). Of course, more porosity certainly affects the hydrophobicity of the membrane and makes the membrane hydrophilic. It is also the size of the pores that decreases with increasing porosity. In general, there is a competition between these three parameters and at one point we will have the highest efficiency for each value of these three parameters.

The question may be asked why the amount of porosity increases with increasing additive and the size of cavities decreases. The reason is that by adding the additive to the system, the first part of the process is phase separation (i.e., the formation of finger structure in the upper layer of the membrane) and to some extent the length of the finger structure increases, but our discussion goes back to the post-finger structure, the spongy state. At this point, the additive causes high porosity with small cavities, a result that the table above confirms. This can be seen by looking closely at the SEM images. In fact, the additive affects both parts of the membrane structure, i.e. the finger structure and its density, so with the addition of the additive, the length of the fingers increases, but the cavities of the dense structure become smaller, so the porosity of the dense part increases.

CONCLUSION

In this paper, the effect of various parameters such as PVDF polymer concentration, solvent types, different additives, and coagulation bath temperature on the phase separation step on the structure and morphology of membranes fabricated from polyvinylidene fluoride are investigated. The results revealed that the phase separation rate of various solvents has the order of NMP<DMF<DMAc. It means the phase separation process

performed earlier using NMP as a solvent, which indicates that the viscosity of solutions made with NMP solvent is lower than DMF and DMAc. According to the experimental data, there is high solubility and high phase separation rate in the water and NMP solution, leading to the macro-cavities structure. Also, tear-like cavities between water and DMF, and finger-like cavities between water and DMAc are observed. It can be concluded that the significant difference in solubility parameter between the polymer and the solvent, which means higher solubility, is resulted in macro cavity structure. Moreover, it is proved that the structure of the membrane is changed from tear-like cavities at low concentrations to regular finger cavities at medium concentrations and by a further increase of concentration, the finger-like cavities are placed more regularly next to each other. At a concentration of more than 30 wt% of the dense structure polymer, macro cavities are formed due to the entrapment of water solvent in the inner structure of the membrane. By decreasing the coagulation bath temperature, the phase separation process becomes slower, which resulted in a membrane with higher porosity and smaller pore size. As the temperature increases, due to the faster phase separation process, the morphology of the membrane changes towards a macro cavities structure with less porosity. The polymer type is very decisive on the membrane formation behavior. For polyurethane sulfonate, the increase of temperature leads to a porous structure, and the decrease of temperature leads to a dense structure. In contrast, PVDF polymer showed an opposite behavior toward temperature changes, which is attributed to the hydrophobicity of this polymer type. To investigate the effect of additives, three-phase diagrams in the presence of dimethyl acetate solvent and SEM images have been examined. The results show that the addition of polyethylene glycol abnormally increases the viscosity of the solution since polyethylene glycol has a higher molecular weight than other additives. Accordingly, the kinetics of separation decreases, leading to a dense structure, less porosity and larger pore size. For additives with lower molecular weight, such as acetic acid and methanol, binodal has the largest distance from the polymer-solvent axis and the phase separation process is fast; hence, it has the least instability and a more porous structure than other additives.

REFERENCES

1. Bakeri G, Ismail AF, Shariaty-Niassar M, Matsuura T. Effect of polymer concentration on the structure and performance of polyetherimide hollow fiber membranes. J Membr Sci. 2010;363(1-2): 103-111.
2. Bakeri G, Ismail AF, Rana D, Matsuura T. Development of high performance surface modified polyetherimide hollow fiber membrane for gas–liquid contacting processes. Chem Eng J. 2012;198:327-337.
3. Oshima KH, Evans-Strickfaden TT, Highsmith AK, Ades EW. The use of a microporous polyvinylidene fluoride (PVDF) membrane filter to separate contaminating viral particles from biologically important proteins. Biologicals. 1996;24(2):137-145.
4. Tan X, Tan SP, Teo WK, Li K. Polyvinylidene fluoride (PVDF) hollow fibre membranes for ammonia removal from water. J Membr Sci. 2006;271(1-2):59-68.
5. Munari S, Bottino A, Capannelli G. Casting and performance of polyvinylidene fluoride based membranes. J Membr Sci. 1983 ; 16:181-193.
6. Wu B, Li K, Teo WK. Preparation and characterization of poly (vinylidene fluoride) hollow fiber membranes for vacuum membrane distillation. J Appl Polym Sc. 2007;106(3):1482-1495.
7. Uragami T, Naito Y, Sugihara M. Studies on synthesis and permeability of special polymer membranes. Polym. 1981;4(10): 617-622.
8. Nohmi T, Yamada T. Polyvinylidene fluoride type resin hollow filament microfilter and process for producing the same. Google patent US 4,399,035. 1983.
9. Shipman GH. Microporous sheet material, method of making and articles made therewith. Google patent United States 4,539,256. 1985.
10. Kang GD, Cao YM. Application and modification of poly (vinylidene fluoride) (PVDF) membranes–a review. J Membr Sci. 2014;463:145-165.
11. Bottino A, Capannelli G, Comite A. Novel porous poly (vinylidene fluoride) membranes for membrane distillation. Desalination. 2005;183(1-3):375-382.
12. Mijović J, Luo HL, Han CD. Property-morphology relationships of polymethylmethacrylate/polyvinylidenefluoride blends. Polym Eng Sci. 1982;22(4):234-240.
13. Noland JS, Hsu NC, Saxon R, Schmitt JM. Compatible high polymers: Poly (vinylidene fluoride) blends with homopolymers of methyl and ethyl methacrylate. ACS Publications. 1971.
14. Stengaard FF. Preparation of asymmetric microfiltration membranes and modification of their properties by chemical treatment. J Membr Sci. 1988;36:257-275.
15. Khodabakhshi AR, Madaeni SS, Xu TW, Wu L, Wu C, Li C, et al. Preparation, optimization and characterization of novel ion exchange membranes by blending of chemically modified PVDF and SPPO. Sep Purif Technol. 2012;90:10-21.
16. Wang L, Magliocca E, Cunningham EL, Mustain WE, Poynton SD, Escudero-Cid R, et al. An optimised synthesis of high performance radiation-grafted anion-exchange membranes. Green Chem. 2017;19(3):831-843.
17. Ghasem N, Al-Marzouqi M, Duidar A. Effect of PVDF concentration on the morphology and performance of hollow fiber membrane employed as gas–liquid membrane contactor for CO2 absorption. Sep Purif Technol. 2012;98:174-185.
18. Pramono E, Simamora AL, Radiman CL, Wahyuningrum D. Effects of PVDF concentration on the properties of PVDF membranes. InIOP Conference Series: Earth and Environmental Science, IOP Publishing. 2017;75(1):012027.
19. Loh CH, Wang R. Effects of additives and coagulant temperature on fabrication of high performance PVDF/Pluronic F127 blend hollow fiber membranes via nonsolvent induced phase separation. Chin J Chem. 2012;20(1):71-79.
20. Cheng LP. Effect of temperature on the formation of microporous PVDF membranes by precipitation from 1-octanol/DMF/PVDF and water/DMF/PVDF systems. Macromolecules. 1999;32(20):6668-6674.
21. Peng J, Su Y, Chen W, Shi Q, Jiang Z. Effects of coagulation bath temperature on the separation performance and antifouling property of poly (ether sulfone) ultrafiltration membranes. Ind Eng Chem Res. 2010;49(10):4858-4864.
22. Wang X, Zhang L, Sun D, An Q, Chen H. Effect of coagulation bath temperature on formation mechanism of poly (vinylidene fluoride) membrane. J Appl Polym Sci. 2008;110(3):1656-1663.
23. Amirilargani M, Saljoughi E, Mohammadi T, Moghbeli MR. Effects of coagulation bath temperature and polyvinylpyrrolidone content on flat sheet asymmetric polyethersulfone membranes. Polym Eng Sci. 2010;50(5):885-893.

24. Fontananova E, Jansen JC, Cristiano A, Curcio E, Drioli E. Effect of additives in the casting solution on the formation of PVDF membranes. Desalination. 2006;192(1-3):190-197.
25. Khayet M, Feng CY, Khulbe KC, Matsuura T. Study on the effect of a non-solvent additive on the morphology and performance of ultrafiltration hollow-fiber membranes. Desalination. 2002;148(1-3): 321-327.
26. Yuliwati E, Ismail AF. Effect of additives concentration on the surface properties and performance of PVDF ultrafiltration membranes for refinery produced wastewater treatment. Desalination. 2011;273(1): 226-234.
27. Li HB, Shi WY, Zhang YF, Liu DQ, Liu XF. Effects of additives on the morphology and performance of PPTA/PVDF in situ blend UF membrane. Polymer. 2014;6(6):1846-1861.
28. Yeow ML, Liu YT, Li K. Morphological study of poly (vinylidene fluoride) asymmetric membranes: effects of the solvent, additive, and dope temperature. J Appl Polym Sci. 2004;92(3):1782-1789.
29. García-Fernández L, García-Payo MC, Khayet M. Effects of mixed solvents on the structural morphology and membrane distillation performance of PVDF-HFP hollow fiber membranes. J Membr Sci. 2014;468:324-338.
30. Karimi A, Khataee A, Vatanpour V, Safarpour M. The effect of different solvents on the morphology and performance of the ZIF-8 modified PVDF ultrafiltration membranes. Sep Purif Technol. 2020;253:117548.
31. Wang X, Zhang L, Sun D, An Q, Chen H. Formation mechanism and crystallization of poly (vinylidene fluoride) membrane via immersion precipitation method. Desalination. 2009;236(1-3):170-178.
32. Cheng LP, Young TH, Fang L, Gau JJ. Formation of particulate microporous poly (vinylidene fluoride) membranes by isothermal immersion precipitation from the 1-octanol/dimethylformamide/poly (vinylidene fluoride) system. Polymer. 1999;40(9):2395-2403.
33. Lin DJ, Beltsios K, Young TH, Jeng YS, Cheng LP. Strong effect of precursor preparation on the morphology of semicrystalline phase inversion poly (vinylidene fluoride) membranes. J Membr Sci. 2006;274(1-2):64-72.
34. Benz M, Euler WB. Determination of the crystalline phases of poly (vinylidene fluoride) under different preparation conditions using differential scanning calorimetry and infrared spectroscopy. J Appl Polym Sci. 2003;89(4):1093-1100.
35. Gregorio Jr R. Determination of the α, β, and γ crystalline phases of poly (vinylidene fluoride) films prepared at different conditions. J Appl Polym Sci. 2006;100(4):3272-3279.
36. Madorsky SL. Thermal degradation of organic polymers. Interscience Publishers, New York. 1964;117.
37. Nguyen T. Degradation of poly [vinyl fluoride] and poly [vinylidene fluoride]. Polymer Rev. 1985;25(2):227-275.
38. Lovinger A, Reed D. Inhomogeneous thermal degradation of poly (vinylidene fluoride) crystallized from the melt. Macromolecules. 1980;13(4):989-994.
39. Furusho N, Komatsu T, Nakagawa T. A Study of the Thermal Degradation of Several Halogen-containing Polymers by Torsional Braid Analysis. Bull Chem Soc Jpn. 197447(7):1573-1577.
40. Benzinger WD, Parekh BS, Eichelberger JL. High temperature ultrafiltration with Kynar® poly (vinylidene fluoride) membranes. Sep Sci Technol. 1980;15(4):1193-1204.
41. Shinohara H. Fluorination of polyhydrofluoroethylenes. II. Formation of perfluoroalkyl carboxylic acids on the surface region of poly (vinylidene fluoride) film by oxyfluorination, fluorination, and hydrolysis. J Polym Sci A Polym Chem. 1979;17(5):1543-1556.
42. Komaki Y. Growth of fine holes by the chemical etching of fission tracks in polyvinylidene fluoride. Nuclear Tracks. 1979;3(1-2):33-44.
43. Hoa SV, Ouellette P. Stress corrosion cracking of poly (vinylidene fluoride) in sodium hydroxide. Polymer Eng Sci. 1983;23(4):202-205.
44. Kise H, Ogata H. Phase transfer catalysis in dehydrofluorination of poly (vinylidene fluoride) by aqueous sodium hydroxide solutions. J Polym Sci A Polym Chem. 1983;21(12):3443-3451.
45. Vigo F, Uliana C, Cavazza B, Salvemini F. Mechanical, chemical and bacterial resistance of modified polyvinylidene fluoride membranes suitable for ultrafiltration of oily emulsions. J Membr Sci. 1984;21(3): 295-306.
46. Hashim NA, Liu Y, Li K. Stability of PVDF hollow fibre membranes in sodium hydroxide aqueous solution. Chem Eng Sci. 201;66(8): 1565-1575.
47. Sukitpaneenit P, Chung TS. Molecular elucidation of morphology and mechanical properties of PVDF hollow fiber membranes from aspects of phase inversion, crystallization, and rheology. Hollow Fiber Membranes, Elsevier. 2021:333-360.
48. Bottino A, Camera-Roda G, Capannelli G, Munari S. The formation of microporous polyvinylidene difluoride membranes by phase separation. J Membr Sci. 1991;57(1):1-20.
49. Shih HC, Yeh YS, Yasuda H. Morphology of microporous poly (vinylidene fluoride) membranes studied by gas permeation and scanning electron microscopy. J Membr Sci. 1990;50(3):299-317.
50. Li Q, Xu ZL, Yu LY. Effects of mixed solvents and PVDF types on performances of PVDF microporous membranes. J Appl Polym Sci. 2010;115(4):2277-2287.
51. Bottino A, Capannelli G, Munari S, Turturro A. High performance ultrafiltration membranes cast from LiCl doped solutions. Desalination. 1988;68(2-3):167-177.
52. Kong J, Li K. Preparation of PVDF hollow-fiber membranes via immersion precipitation. J Appl Polym Sci. 2001;81(7):1643-1653.
53. Khayet M, Matsuura T. Preparation and characterization of polyvinylidene fluoride membranes for membrane distillation. Ind Eng Chem Res. 2001;40(24):5710-5718.
54. Presser V, McDonough J, Yeon SH, Gogotsi Y. Effect of pore size on carbon dioxide sorption by carbide derived carbon. Energy Environ Sci. 2011;4(8):3059-3066.
55. Wang R, Li DF, Zhou C, Liu M, Liang DT. Impact of DEA solutions with and without CO2 loading on porous polypropylene membranes intended for use as contactors. J Membr Sci. 2004;229(1-2):147-157.
56. Mansourizadeh A, Ismail AF, Abdullah MS, Ng BC. Preparation of polyvinylidene fluoride hollow fiber membranes for CO2 absorption using phase-inversion promoter additives. J Membr Sci. 2010;355(1-2): 200-207.
57. Li KA. Designing asymmetric PVDF hollow fibres for soluble gas removal. Chem Eng Technol. 2002;25(2):203-206.
58. Hernandez Y, Lotya M, Rickard D, Bergin SD, Coleman JN. Measurement of multicomponent solubility parameters for graphene facilitates solvent discovery. Langmuir. 2010;26(5):3208-3213.
59. Liu F, Zhu BK, Xu YY. Improving the hydrophilicity of poly (vinylidene fluoride) porous membranes by electron beam initiated surface grafting of AA/SSS binary monomers. Appl Surf Sci. 2006;253(4):2096-2101.
60. Lovinger AJ. Annealing of poly (vinylidene fluoride) and formation of a fifth phase. Macromolecules. 1982;15(1):40-44.
61. Mansourizadeh A, Ismail AF. Effect of additives on the structure and performance of polysulfone hollow fiber membranes for CO2 absorption. J Membr Sci. 2010;348(1-2):260-267.
62. Mansourizadeh A. Experimental study of CO2 absorption/stripping via PVDF hollow fiber membrane contactor. Chem Eng Res Des. 2012;90(4):555-562.
63. Shi L, Wang R, Cao Y, Liang DT, Tay JH. Effect of additives on the fabrication of poly (vinylidene fluoride-co-hexafluropropylene)(PVDF-

HFP) asymmetric microporous hollow fiber membranes. J Membr Sci. 2008;315(1-2):195-204.

64. Naim R, Ismail AF, Mansourizadeh A. Effect of non-solvent additives on the structure and performance of PVDF hollow fiber membrane contactor for CO2 stripping. J Membr Sci. 2012;423:503-513.